Peer-reviewed preprint submitted to EartArXiv. The manuscript is part of Chapter 5.4 of
The Encyclopedia of Volcanoes, 3rd Edition, Elsevier
Edited by C. Bonadona, L. Caricchi, A. Clarke, P. Cole, J. Lindsay, J. Lowenstern, R. Robertson and M. L. Villega

Volcano flank instabilities and lateral collapse.

Lucia Capra*, Instituto de Geociencias, Universidad Nacional Autónoma de México, 76230, QRO, México
Alexander Belousov, Institute of Volcanology and Seismology, Petropavlovsk-Kamchatsky, Russia.
Benjamin Bernard, Instituto Geofísico, Escuela Politécnica Nacional, Ladrón de Guevara E11-253 y Andalucía, Quito, Ecuador.
Anja Dufresne, RWTH Aachen University, Department of Engineering Geology and Hydrogeology, Lochnerstr. 4-20, 52064 Aachen, Germany
Anne Le Friant, Institut de Physique du Globe de Paris - Université Paris Cité, 1, rue Jussieu, 75238 Paris Cedex 05.
Engielle Mae R. Paguican, Department of Geography, King's College London, London, UK.
Matteo Roverato, BIGEA Department, Alma Mater Studiorum, University of Bologna, Italy.
Benjamin van Wyk de Vries, Université Clermont Auvergne, Observatoire du Physique du Globe de Clermont, Laboratoire Magmas et Volcans, UMR6524-CNRS.
Sebastian F.L. Watt, School of Geography, Earth and Environmental Sciences, University of Birmingham, UK.
*Corresponding author: lcapra@geociencias.unam.mx

Abstract.

The gravitational instability and subsequent lateral collapse of a volcano is a common phenomenon observed in most types of volcanoes, from continental to oceanic environments. Both intrinsic and extrinsic factors contribute to volcanic collapse, including the volcano's internal structure, geological setting, and a range of volcanic and non-volcanic processes, including climatic conditions.
Lateral collapse typically leaves a scar on the volcano's flank and produces a corresponding debris avalanche deposit. Debris avalanched deposits are characterized by distinct morphological features and internal facies that can reveal the causes of the instability and the interaction of the failure mass with the surrounding substrate and landscape. Lateral collapses can trigger secondary hazards such as magmatic and phreatic eruptions, tsunamis, lahars, river obstructions with the formation of natural dams, and submarine landslides, leading to potentially catastrophic environmental effects.
Studying volcanic landslides is fundamental for improving our scientific knowledge of this geological process and understanding their associated hazards in the short and long term. Such knowledge can enhance social awareness, promoting urban resilience and ecosystem protection.

Key words.

Volcanic lateral collapse, flank instability, volcanic landslides, volcanic debris avalanche, volcano spreading, debris avalanche facies, hummock, jigsaw crack.

Introduction.

The gravitational failure of volcanic slopes, starting with landsliding and generating volcanic debris avalanches, is a natural phenomenon that has been recognized on volcanoes worldwide, and in extraterrestrial examples such as Olympus Mons on Mars. These lateral collapse processes (i.e., volcanic landslides, as a more generic term) can affect active or dormant volcano edifices, from stratovolcanoes and shield volcanoes to simple cinder cones, in aerial to submarine environments, and are globally distributed, irrespective of the volcano composition or geodynamic setting (Box 5.4.1) [1]. Several historical events, including those that have caused hundreds of deaths, have been documented since the 18th century, but the direct observation of the 1980 Mount St. Helens (USA) eruption in particular advanced scientific knowledge of the factors promoting volcano flank instability, triggering mechanisms, and the characteristics of associated deposits.

All volcanoes can fail under gravitational forces if strained by destabilizing factors. These factors are not necessarily eruption-related, and close monitoring is necessary to detect potential signs and causes of changing slope stability. Failure may be driven or accelerated by climatic factors or earthquakes, and the regional tectonic framework may also influence edifice stability, failure style and direction [E1, 2]. Edifice failure can induce sudden, deep-seated and large volume (up to tens of cubic kilometers) movements, with progressive fragmentation leading to transport of debris at velocities reaching tens of meters per second, distributing deposits for tens of kilometers, with catastrophic effects on the landscape. The geomorphologic characteristics of this process are distinctive, with a landslide scar commonly encompassing a sector of the former volcanic summit and flank, and the downslope debris avalanche deposit typically displaying a hummocky (mound-like) surface. Volcanic debris avalanche deposits can be spectacular in outcrop scale, with chaotic, multicolored textural features resembling a puzzle comprising intact portions of the volcano, which make them easily distinguishable from other volcaniclastic deposits, such as those from pyroclastic density currents or lahars (Part 3 Chapters 4.4 and 5.1). Textural and lithological features of the deposit can help to identify the main causes of failure. Lateral collapse can directly affect the underlying magmatic system due to the rapid decompression of shallow magma bodies, potentially leading to energetic eruptions contemporaneous with or just after the collapse and with potential long-term effects on the structure and eruption rate of feeding systems. Secondary effects include tsunamis, lahars, and the formation of temporary lakes due to drainage blockage, with associated environmental and ecosystem impacts due to landscape burial, vegetation loss and hydrological effects.

Box 5.4.1. Debris avalanche world database.

Database detailing volcanic debris avalanche deposits from 594 volcanoes across 52 countries. Approximately half of these deposits are situated in Japan, the Americas, and Russia. Since 1500 AD, there have been 28 documented edifice collapses with deposit volumes ≥0.1 km^3, averaging more than 5 events per century. A significant majority of these collapses were linked to explosive magmatic eruptions, primarily ranging from VEI (Volcanic Explosivity Index; Part 3, Chapter 2.7) 4 to 5. Some single volcanoes, such as Piton de Neiges (Indian Ocean), Taranaki (New Zealand), Shiveluch (Kamchatka, Russia), Harimkotan (Kurile Islands, Russia) and Augustine (Alaska), have experienced multiple lateral collapses and appear to be prone to repeated cycles of growth and failure [1].

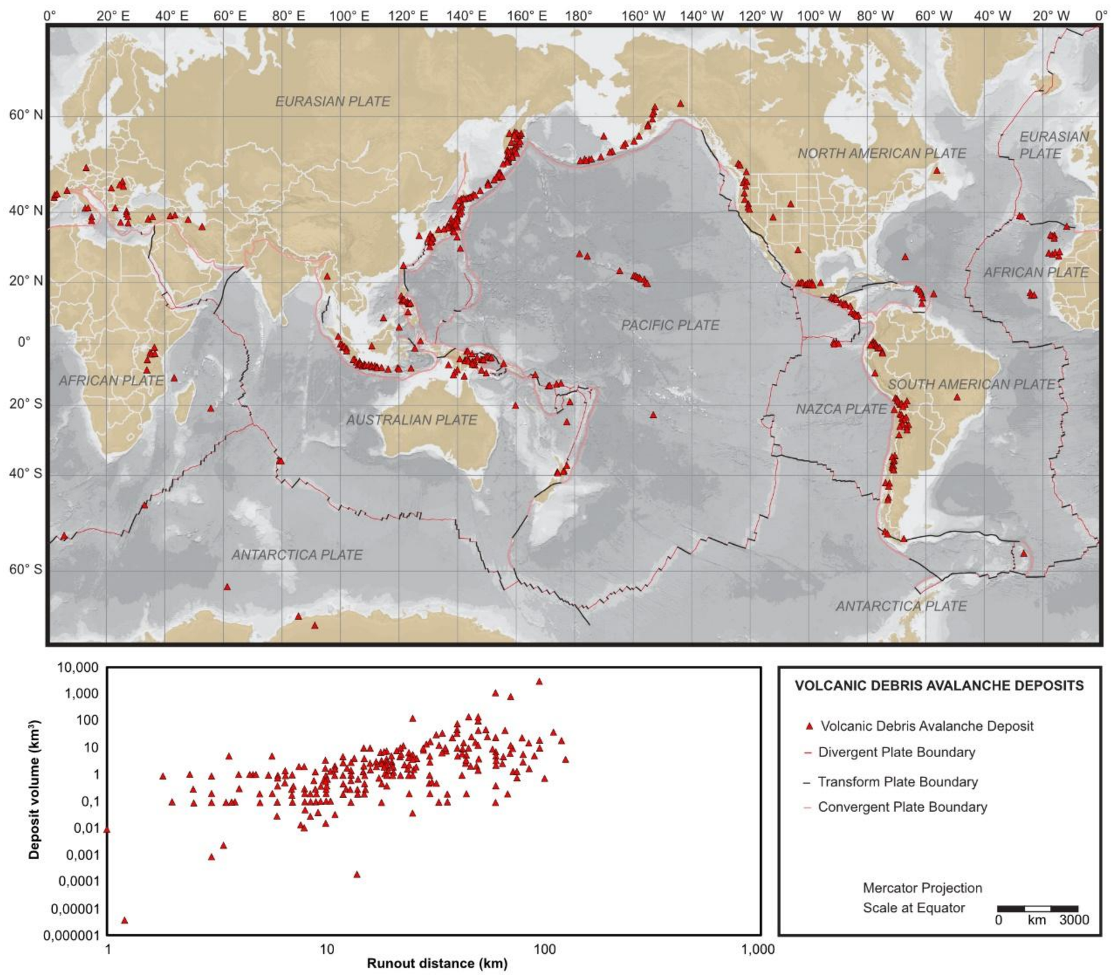

Figure BOX 5.4.1. Distribution of volcanoes that have produced debris avalanche deposits. Note that Holocene and older volcanoes are included in this database [1]. The plot shows the relationship between VDA volume and runout distance. The map is modified after [1]; the locations of Holocene volcanoes are from the Smithsonian Institution's Global Volcanism Program, and all others are from relevant publications and internet research.

The process: From volcanic landslides to volcanic debris avalanches.

The structure and stability of any individual volcano is unique and determined by its evolution, setting and local environmental conditions, meaning that a single predictive model to explain edifice instability and landslide characteristics is unlikely. Nevertheless, several intrinsic and extrinsic factors can interplay to promote volcano lateral collapse.

Factors contributing to volcano instability.

The long-term vertical growth of volcanic edifices is limited by several factors that result in gravitational instabilities. As a result, many long-lived volcanoes will undergo multiple flank (the partial failure of a volcano slope) or sector (including the volcano summit) collapses during their lifetime, at recurrence rates of hundreds to tens of thousands of years. Several volcanic and non-volcanic processes can accelerate the destabilization of volcanoes and act as trigger mechanisms for collapse [3].

Intrinsic factors

These factors are involved in volcano construction (Figure 5.4.1) [3]. Volcanoes are constructed by the accumulation of volcanic deposits, a process that can last from a few hours for small monogenetic edifices to millions of years for complex polygenetic volcanoes. Their building material consists of lava and volcaniclastic deposits, with varied cohesion, angle of internal friction and rock (mass) strengths. These materials are also intruded by dikes and sills. This leads to sharp discontinuities in strength, porosity and permeability, often at high angles, producing mechanically heterogeneous structures. In addition, mechanical and chemical alteration due to hydrothermal activity and magmatic intrusion can pressurize and weaken the core of the edifice during and beyond volcanic activity. Hydrothermal alteration generally leads to deep-seated landslides (Box 5.4.2). Volcano morphology is also modified by eruptive processes and these, along with lateral collapses, create topography and internal slide surfaces that control future growth patterns and instability. The inherited influence of past failures can lead to repeating events that typically decrease in size through time. As volcanoes expand, vent migration often results in asymmetric growth. Lastly, magmatic differentiation and changes in eruptive dynamics and rate have also been recognized as factors driving instability [4]. Detailed geological study of the landslide scars and analysis of debris avalanche deposits can help reconstruct the intrinsic factors affecting volcano instability.

Extrinsic factors

Extrinsic factors can be grouped into four categories (Figure 5.4.1) [3]. (1) The nature of the volcano's basement, known as the geological setting, controls in part how the volcano can deform under its own weight. The competence and structure of the basement rock formations, including the presence of weak or dipping substrata, can promote gravitational spreading and instability (e.g. Socompa volcano, Chile; [5]). Failure of the substratum is often associated to V-shaped landslide scars (e.g. Mombacho volcano, Nicaragua; Box 5.4.2) [6]. (2) The geodynamic setting, corresponding to the tectonic stresses applied to the basement and the volcano, can affect volcano morphology by controlling the preferential direction of intruding magma and by deforming it along with the basement. Both the edifice morphology and stress field can influence collapse directions, which are often parallel or perpendicular to regional fault systems [E1]. (3) The topographic setting, referring to the slope and aspect of the volcano's basement, is a major unconformity. Poor coupling and/or steep dip of this unconformity influence both the growth and stability of the volcano. The influence of the topographic setting is highlighted by the preferential direction of large landslides originating from volcanoes located on the edge of topographic ridges and cordilleras (e.g. Citlaltépetl volcano, México; Shiveluch, Russia; Sangay, Ecuador). (4) The climatic setting can affect the stability of the volcanic edifice through static load changes, weathering, and erosion [7]. Climatic drivers affecting slope stability include glacier retreat, permafrost degradation, increase in water circulation, and change in sea level. Permafrost degradation and water circulation will enhance chemical weathering, erosion, and pore pressure, all reducing rock strength (e.g., Meager, Canada; Mt Rainier, USA; Nevado del Huila, Colombia). Potential relationships between volcano instability and local sea-level change have been proposed, linked to periods of rapid erosion and debuttressing of volcano flanks (i.e. Tenerife, Spain), to loss of edifice strength via pore fluid pressurization and/or hydrothermal activity during sea-level rise (i.e Lesser Antilles; Hawaii, USA), or to subsurface stress field changes and deformation that influence magma ascent and eruption (i.e. Planchón-Peteroa, Chile).

Triggering mechanisms.

Trigger mechanisms are short-term or final phenomena preceding lateral collapse, although a single trigger is not always identifiable, particularly for pre-historic events. The most common triggers are linked to intrusions or eruptions, associated with rapid changes in the volcano's center of mass and/or a loss of strength from volcano-tectonic earthquakes or enhanced hydrothermal activity. Intrusion and eruption can often produce deep-seated failure, while the rapid accumulation of volcanic deposits generally causes shallow landslides. Non-volcanic triggers include tectonic earthquakes, which can weaken edifices and load slopes prone to failure, influenced by pre-existing faults or discontinuities, and meteorological events, particularly those associated with intense rainfall, which promote slope failure through increased pore fluid pressure.

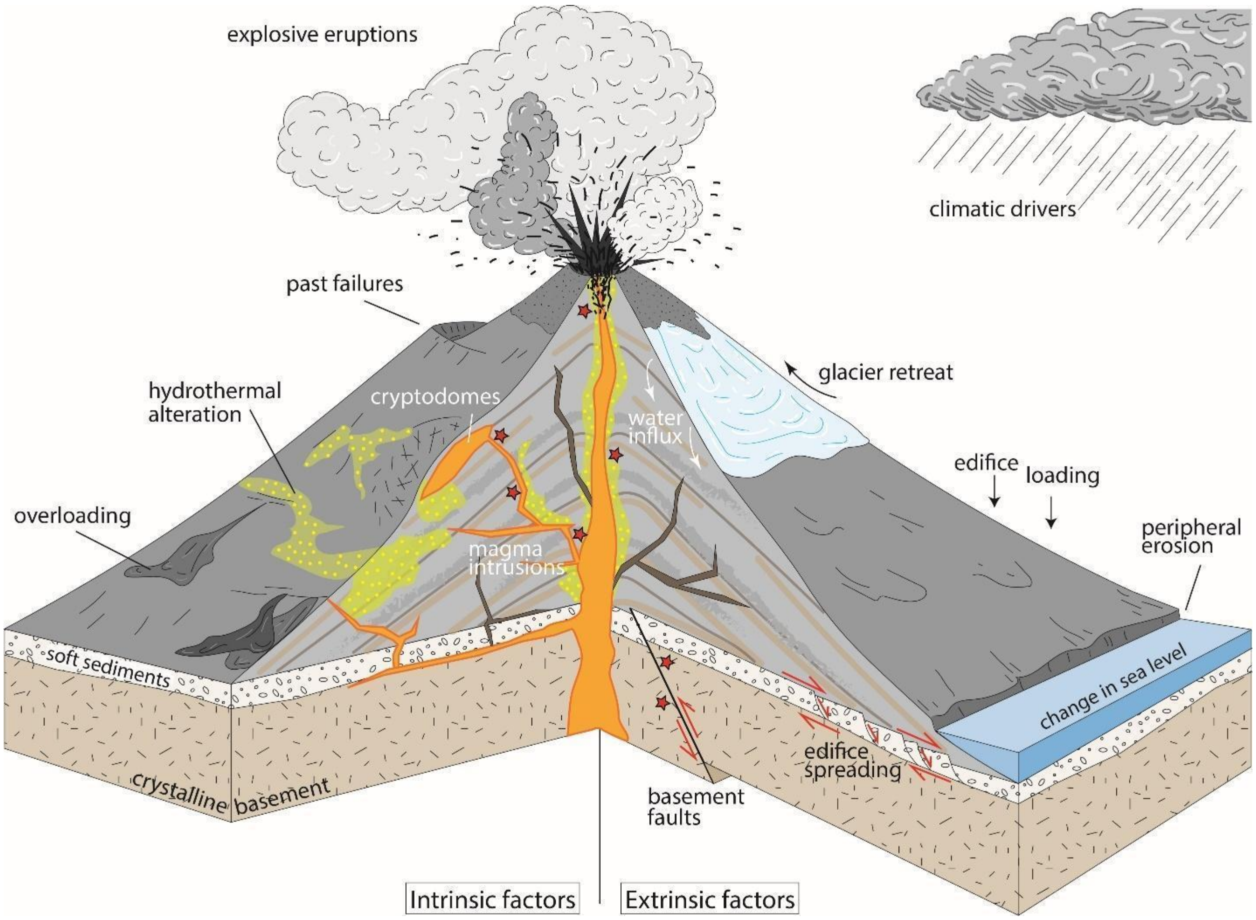

Figure 5.4.1 Sketch representation of the intrinsic and extrinsic instability factors that can destabilize a volcano. Red stars represent volcano-tectonic and deformation seismicity. See the text for more details. The figure is modified after [3].

Box 5.4.2. Mombacho volcano landslides.

Mombacho (Nicaragua) is a globally representative type-example for volcano landslides. It is a medium-sized composite volcano, built mainly of andesitic lava flows and pyroclastic deposits. It has two young major lateral collapse amphitheaters and avalanche deposits [6]. Around AD 300, the El Crater landslide occurred on the mid-upper slopes due to severe internal hydrothermal alteration, leaving a bowl-shaped scar and dispersing deposits for 12 km from the source. In AD 600, the Las Isletas landslide formed on the northeast flanks, entering Lake Nicaragua and forming an archipelago of hundreds of islands. In this event, the volcano failed on a stratigraphic plane of weakness, forming a triangular shaped scar, with an inclined floor. The deposit is composed of fresh lava and pyroclastics alongside material derived from deeper substrata. Las Isletas is interpreted as developing through slow gravitational spreading on this weak substrata, before sudden acceleration. El Crater, in contrast, developed through long-term hydrothermal weakening, with spreading and faulting facilitating internal fracturing and hydrothermal circulation; the climatic setting of tropical cloud forest with high rainfall fed this system. For both landslides, seismic activity may have promoted failure. An older collapse, the

Dante deposit, is found to the SE of the volcano and there are two other smaller landslides (Figure Box 5.4.2).

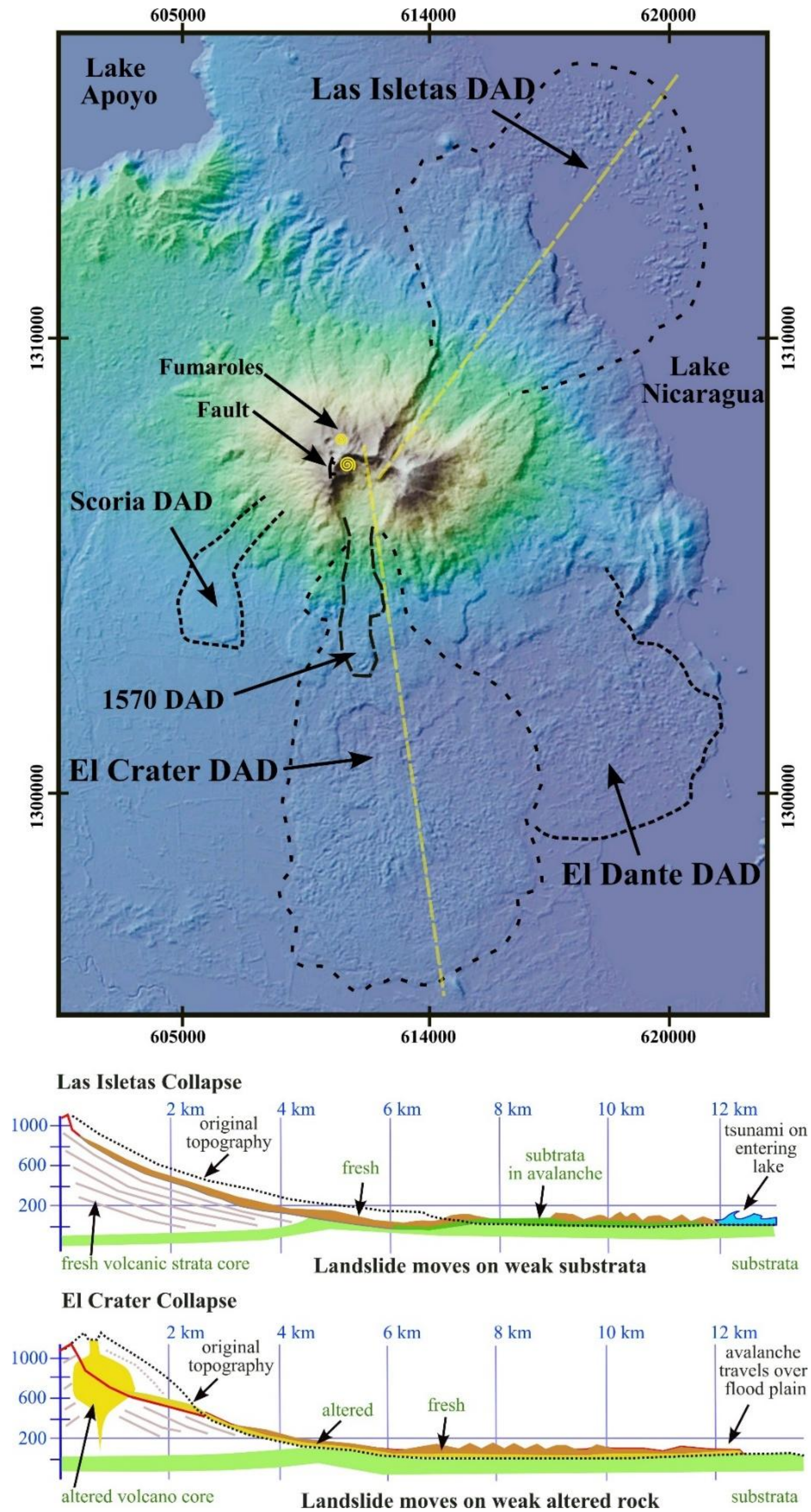

Figure Box 5.4.2. (top) Shaded relief and altitude image from Copernicus 30 m DEM of Mombacho volcano (Nicaragua) with El Crater and Las Isletas debris avalanche deposits (DAD, outlined by black dotted lines). Their landslide scars are clearly visible, as is the internal hummocky terrain. The 1570 debris avalanche deposit is shown, as well as a smaller scoria landslide and the much older El Dante deposit. (bottom) Simplified sketch of the origin and evolution of lithologies of El Crater and Las Isletas debris avalanche deposits (yellow dotted line cross section). The position of active fumaroles is shown as a yellow spiral and a potential landslide scar is shown by a small fault symbol on the west side of El Crater.

Instability remains a concern at Mombacho, particularly from smaller volcanic landslides. In 1570, an avalanche-debris flow from the walls of El Crater destroyed the original town of Mombacho. The El Crater fumaroles have recently become more active, changing composition and increasing in extent. A conspicuous fault to the west of the scar has the potential for a landslide on the order of tens of millions of cubic meters, and the scar is now also a site for degassing, as seen by reduced vegetation (Figure Box 5.4.2).

The deposits.

Volcanic debris avalanches: recognition, morphology, texture and sedimentology

The earliest descriptions of deposits resulting from volcano collapse and other mass movements (dry mudflows, debris avalanches, volcanic landslides) go back to events at Raung, Indonesia, Bandai-San, in 1888, and other Japanese volcanoes, Bezymianny, Kamchatka, in 1956, and Katmai-Novarupta, Alaska, in 1912. Yet it was not until 1980, when the Mount St. Helens collapse was directly observed and documented, that the origin and emplacement processes of volcanic debris avalanche deposits became internationally recognized [2].

In many regions, evidence of past collapses and their deposits remains poorly documented. Given the extensive size of volcanic debris avalanche deposits, remote sensing techniques hold strong potential in identifying the distinctive morphological features and spectral properties of these deposits, mapping their extent and, consequently, better understanding their emplacement processes.

The source area of debris avalanche deposits often shows a scar structure with a wide breach to one side. From this breach, hummocks and ridges spread, where unobstructed, radially outwards across the landscape and become successively smaller with distance (Figure 5.4.2) [8]. The spreading of volcanic debris avalanches is at least partially accommodated by listric normal faults resulting in an irregular surficial topography marked by elevated hummocks, whose morphology is modified further by spreading, dewatering, or by contemporaneous volcanic processes (e.g., lahars or tephra deposition) and subsequent erosion.

Large, backward rotational toreva blocks at the base of the breach are a typical feature; so-called after the Toreva landslide in Arizona, where they were first described [9]. These almost intact blocks of the original edifice can be up to several kilometers wide and some hundreds of meters high. Preservation of source stratigraphy, despite internal deformation, is a typical feature of such deposits and is found not only for torevas but also for larger blocks within distal depositional areas (Figure 5.4.2). In volcanoes surrounded by irregular topography, debris avalanches may enter deep valleys, have longer runouts (>45 km) than unconfined ones, and result in thicker deposits (>50 m) with elongated, flow-parallel hummocks, as well as megaclast-rich lithofacies farther down the valley [2].

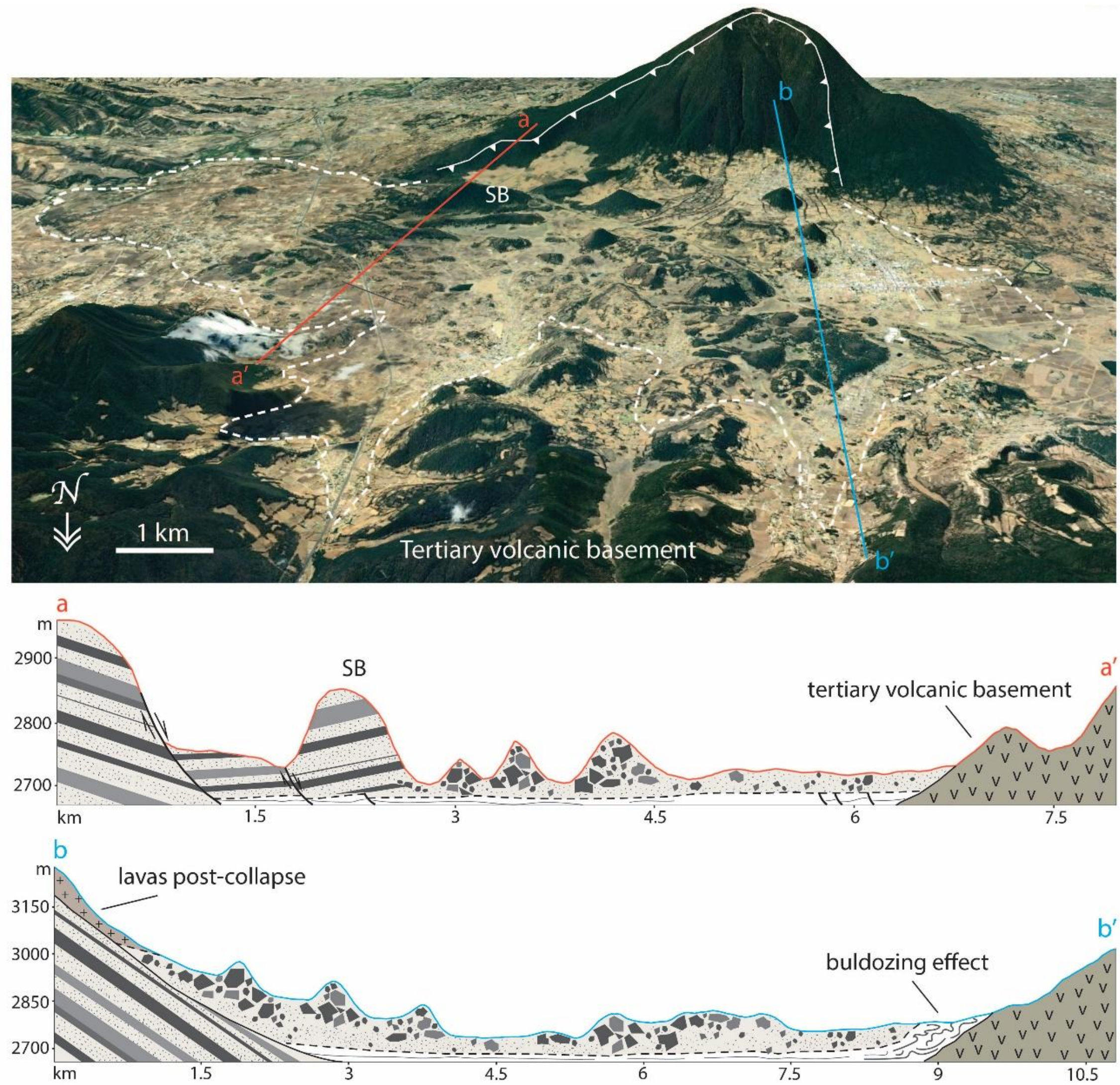

Figure 5.4.2. (top) View from the south of the Jocotitlán volcano (México), and the debris avalanche deposit that resulted from the 9.6 k B.P. sector collapse. (bottom) The eastern flank failure was driven mainly by the edifice spreading on the weak substrate material; the proximal deposit consists of sliding blocks (SB) that laterally evolved to hummocks until stopped against topographic highs of the Tertiary basement (section a-a'). The sector collapse of the main cone is associated with a block facies deposit, with conical

hummocks, radially spreading, and decreasing in size until they encounter topographic highs where substrate bulldozing can be observed (section b-b’). Vertical exaggeration 2X. Image © GoogleEarth.

Facies description.

The wide variability in source lithologies, failure and emplacement mechanisms produces a corresponding variety of sedimentological characteristics of volcanic debris avalanche deposits. Fourteen distinct facies have been recognised in one descriptive scheme [8], which are dependent on the nature of the failed material. The most widely applied facies model is that of Glicken [10], developed on the Mount St. Helens 1980 deposit, which was a dry avalanche that was mostly channeled down the North Fork Toutle River. The two end-member facies of Glicken’s nomenclature are the block facies and the mixed facies (formerly named ‘matrix’ facies, but later renamed by [10] to avoid confusion with the sedimentological definition of ‘matrix’) (Figure 5.4.3). Mapping of these facies revealed large-scale distributional patterns that served to interpret flow phases, travel paths and relative velocities, and to reconstruct the evolution of the entire events, from failure and synchronous eruption through to deposit emplacement.

The block facies generally consists of coherent, unconsolidated to poorly consolidated fragments of the source volcano (up to >100-m across) that are relatively intact in their stratigraphy, with some structural deformation and jigsaw-fractures. These materials can be highly brecciated into a fine sand- to silt-sized matrix and can be a complete gradation between block facies and mixed facies (Figure 5.4.3).

The mixed facies is a highly variable unsorted, ungraded, and unstratified mixture of all rock types from the collapsed edifice, including juvenile materials, and fragments of the substrata (sediments, wood, soil). Particle sizes are usually <0.25 m but can contain several-meter-sized fragments embedded in a polylithologic matrix (Figure 5.4.3) [8].

Another facies model emerged for partially water-saturated debris avalanches in the mostly unconfined runout settings on the ring plains around Mt. Taranaki in New Zealand. Lithofacies descriptions are used to emphasize the lithological attributes of each mapping unit [8]. Three distinct lithofacies exist in this model (axial-A, axial-B, and marginal lithofacies), based on internal structure (decrease in clasts content from axial-A to axial-B, up to 90% of matrix in the marginal lithofacies) and surface morphology (decrease in mounds highs from axial-A to axial-B up to a flat surface for marginal lithofacies), and occupy discrete positions within the deposits. Due to the large amounts of fine-grained material already present in the source lithologies of these events, especially in regions affected by extensive hydrothermal alteration, direct transformation from debris avalanches to cohesive debris flows are common in these types of lateral collapses, and reflected in their deposit characteristics (Part 3, Chapter 5.1).

Regardless of facies model and avalanche type, the basal contacts show distinctive features. A basal facies varies in thickness from a few millimeters to several meters and consists of a mixture of avalanche and substrate material. The contact to in-situ substrate is typically sharp, can be planar, undulating or grooved, and may even feature sheared-off rocks from the substrate. Folding, faulting, shearing, clastic dykes and diapirs often exist at this contact, propagating into the avalanche deposit, and may record syn-movement deformation. Rip-up clasts and fluidized substrate may be incorporated high into deposits, due to ongoing transport, and flame-injections indicate continued (local) movement and deformation during deposit emplacement or stationary overload akin to aggradational (e.g., deltaic) deposits (Figure 5.4.3) [8].

Grain sizes, shapes and textures.

The heterogeneity of the source stratigraphy, and variations in fragmentation and disaggregation during transport produce poorly sorted deposits with highly variable grain size distributions.
Microscopic analyses of surface features of sand-sized grains in the deposits have been used to provide a better understanding of particle interaction processes during transport [2, 8]. Grain morphologies are generally highly irregular, including elongated or spherical shapes and rounded or sharp edges with multiple corners. Surface textures consist of different types of fractures, percussion marks, staircase geometry, broken crystals, scratches of different intensity, lips, parallel grooves, and ridges. Microfractures, percussion marks, and broken crystals represent punctual, rapid inter-particle contacts, indicating that grains moved with some degree of freedom and interacted predominantly by collision. On the other hand, parallel ridges, parallel grooves, scratches, and lips may indicate prolonged interaction between particles, suggesting a more constrained environment.

a
reworked
block facies of fractured
volcanic strata
b
highly-fractured
lava blocks
c
coarse fractured
block facies
clastic dykes
d
jigsaw crack
30 cm
e
reworked
mixed facies
rounded clasts incorporated
from the subtratum
f
40 cm

Figure 5.4.3. Textural features of volcanic debris avalanches deposits. a) Block facies exposure, with a chaotic arrangement of blocks of fractured lavas (dotted lines) and pyroclastic sequences (Nevado de Toluca, Mexico); b) Block facies with a highly fractured lava blocks (dotted lines), some of them highly shattered (Tonila debris avalanche deposit at 6.5 km from the source, Volcán de Colima, Mexico); c) Injections (clastic dikes) of a fluidized basal unit into a coarse fractured block facies (El Zaguan volcanic debris avalanche deposit, Nevado de Toluca, Mexico); d) Close up of a lava fragment showing jigsaw crack texture: e) Mixed facies showing clasts embedded in a homogeneous fine matrix; some rounded clast (white arrows) represent clasts incorporated from the substrate (Tonila debris avalanche deposit at 15 km from the source, Volcán de Colima); f) Block facies showing pervasive hydrothermal alteration (Nevado de Colima, México).

Instability in volcanic islands and marine environments.

Scale and geometry:

In common with terrestrial settings, partially and fully submerged volcanic landforms are also prone to volcanic landslides and catastrophic mass wasting. These events have a particular significance due to their potential for tsunami generation (Part 4, Chapter 3.3), because of their capacity for increased volume and runout via mobilization of seafloor sediment during their transport (substantially expanding their spatial impact), and simply because of the scale of some volcanic island landforms, which makes them host to some of the largest mass movements on Earth (Figure 5.4.4).

Instabilities on and around volcanic islands are a ubiquitous process, evident from morphological scars and deposits in marine volcanic environments that span a wide spectrum of dimensions and slope gradients. In the largest cases, deposits can contain several thousands of cubic kilometers of mobilized material [11] and can extend over hundreds of kilometers in distance, far exceeding the volume and runout of the largest subaerial debris avalanche deposits. Across examples in both oceanic intraplate settings, such as offshore the Hawaiian Archipelago, La Réunion, and the Canary Islands [11], and subduction settings, such as the Lesser Antilles [12], submarine debris avalanche deposits have similar morphological features, which are also shared with their subaerial equivalents. This suggests that similar processes control volcano instability and landslide behavior across all these environments. However, the potential for substrate interaction and secondary failure, triggered by initial volcanic debris avalanche emplacement, is enhanced in submarine environments and has been widely identified [12].

Role in island morphological development.

Volcanic island and seamount morphology can be strongly influenced by mass-wasting processes. Emergent and near-vent landforms commonly show horseshoe structures with wide opening angles as observed in historical lateral collapses (e.g., Anak Krakatau, Indonesia, 2018; Ritter Island, Papua New Guinea, 1888), which may span the land to sea interface and influence subsequent vent positions and the accumulation of products, in turn affecting future instabilities. Debris avalanche and other mass-wasting deposits can accumulate thick volcaniclastic aprons around volcanic islands, often on submerged flanks (e.g., La Réunion). More distally, longer-runout deposits and secondary seafloor sediment failures can leave a widespread imprint of mass wasting processes in adjacent basins [12].

A range of island-flank morphologies suggests that failures may include both gradual and rapid phases, from the deep-seated slumps particularly evident around some ocean islands, such as Hawaii, to much more rapid phases of movements. Long-lived, fault-bound slumps have been linked to gravitational spreading and may be facilitated by island construction on marine sedimentary substrates and by elevated construction rates. As with the other previously described gravitational collapse processes, slumps form distinctive scars but are not associated with rapid, catastrophic phases of movements [13]. More rapid and, in many instances, more shallowly seated volcanic landslides occur across all islands and submarine geodynamic settings and produce debris avalanches with similar morphological characteristics to their subaerial counterparts.

Methods and challenges with reconstruction.

Understanding how submarine landslide deposits were emplaced is crucial, since emplacement dynamics determine the magnitude of the associated tsunamis. This has been a source of debate, due to uncertainties associated with slide physics and dynamics to describe how collapsed material enters the ocean, and in terms of whether failure is gradual, staged, or can occur in more catastrophic single-phase events. Historical events (e.g., Unzen, Japan, in 1792 or Anak Krakatau, Indonesia, 2018) attest to the potential for sudden failure and the transfer of landslide energy into the generation of devastating tsunamis (Part 4, Chapter 3.3). Whether this can simply be scaled up to the extremely large-volume collapses of intraplate ocean islands, remains uncertain. Evidence of stacked turbidites in distal deposits offshore the Canary Islands or Lesser Antilles islands implies complex failure processes, but tsunami deposits at high elevations have been used to demonstrate extreme wave magnitudes, implying rapid and catastrophic failure (Figure 5.4.4). Marine geophysical surveys have increased our ability to characterize landslide deposits around volcanic islands and have highlighted the complexity of emplacement processes, particularly those involving substrate interaction. Geophysical observations and sediment cores offshore the Lesser Antilles demonstrate that emplacement of volcanic debris avalanches in marine settings can trigger widespread and voluminous failures of preexisting low-gradient seafloor sediment [12]. The most likely mechanism for generating large-scale seafloor sediment failures appears to be the propagation of a decollement, from proximal areas that are loaded and incised by the overriding avalanche [12, 13]. Primary deposits also show evidence for transformation to secondary debris flows and the triggering of turbidity currents that can extend for hundreds of kilometers.

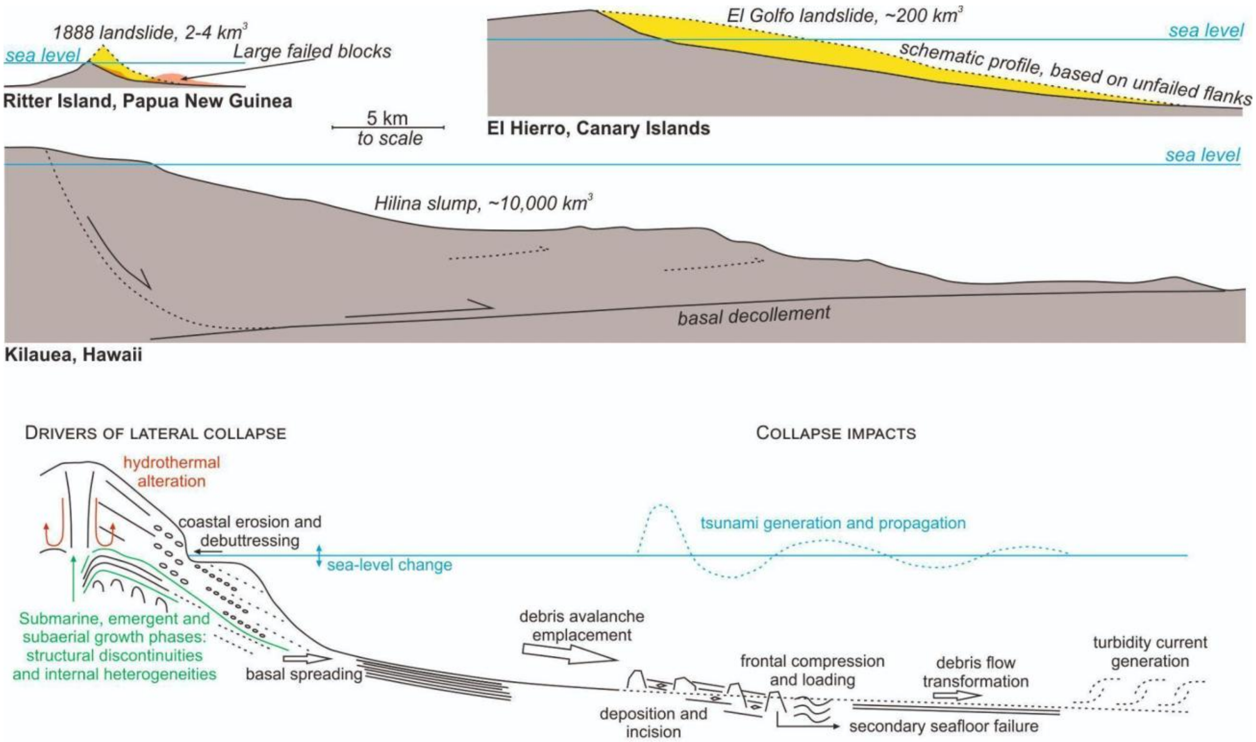

Figure 5.4.4: (top) Cross-section profiles through some examples of volcanic island mass-movements. Ritter Island (island arc) and El Hierro (intraplate) represent examples of large-scale lateral collapses in island settings, generating debris avalanche deposits. El Hierro contrasts with the deep-seated and long-lived Hilina slump on Kilauea, Hawaii, with movement on a basal decollement that may transition to more rapid phases of movement. (bottom) Schematic summary of distinctive features in volcanic-island settings that promote lateral collapse and that distinguish collapse-deposit characteristics, runout and associated hazards.

Volcanic debris avalanche mobility.

The mobility of a debris avalanche is mainly controlled by its initial gravitational potential energy, the downslope topography, internal deformation and basal friction during transport. A general correlation between the volume of the collapsing mass and debris avalanche maximum runout has been proposed (Box 5.4.1), but other factors can enhance mobility. For example, the nature of the source material (e.g. hydrothermal alteration, highly fractured or granular rocks, or the presence of fluids), and the characteristics of the substrate materials influence grain size and bulking, which in turn affects how kinetic energy is dissipated in basal friction, fragmentation and heat loss until the final emplacement. Basal and internal structures, as well as surface morphologies, are evidence of transport and emplacement mechanisms.

Influence of the environment

The sedimentary environment and topography over which a debris avalanche travels, influence how it dissipates kinetic energy until it comes to rest. Obstacles force the debris avalanche to convert some of its kinetic energy into gravitational potential energy, and to consume some of it in the form of frictional loss. Confinement in valleys limits lateral spread and can increase runout by reducing the surface for friction loss and increasing the thickness of the debris avalanche [2]. The slope of the substratum also plays a major role, as it controls the amount of initial gravitational potential energy. Bulking of substrate materials has two opposing effects on avalanche mobility: 1) it dissipates kinetic energy through friction and 2) it increases its volume and, consequently, its intermediate gravitational potential energy. The nature and water content of the entrained materials can modify the mobility of a debris avalanche by adding lubrication to the base or transforming it into a debris flow [8].

Surface morphology and internal structures as evidence of transport and emplacement.

Within volcanic debris avalanche deposits, jigsaw cracked blocks, hummocks, faults, and accumulation ridges are typical features. Jigsaw cracks, primarily formed by unloading of the collapsing mass [10], evolve by progressive fragmentation. The irregular hummocky topography reflects transport conditions including interactions with underlying topography and the initial composition of the failure mass. Hummocks and torevas are the morphological expressions of brittle extension and are related to the strain and deformation regimes within the debris avalanche. Their formation starts as fracturing, as the spreading of the landslide forces the upper brittle layer to split and drop against adjacent blocks. Hummocks tend to become smaller as the debris avalanche spreads farther away from the source area, but they can also form compressional ridges and hummock clusters away from the source and towards the topographic barriers, where fold and thrust structures can form (Figure 5.4.2). In analogue laboratory experiments, elongated hummocks, longitudinal ridges and flow bands are suggested to result from the homogeneously sized and homogeneously competent materials involved [14]. However, in the range of mass movements, their formation is suggested to be an intrinsic tendency of granular material with heterogeneous grain size distribution, and their expression as elongated hummocks, longitudinal ridges or flowbands depends on a combination of material property, external influences, and emplacement velocity [15]. Finally, the accumulation of debris at the front of the distal zone indicates strong frontal deceleration and the bulldozing of substrata along the runout path (Figure 5.4.2).

Emplacement mechanisms

Field observations of debris avalanche morphologies and internal structures have inspired several hypotheses on their dynamic behavior and mobility. None involves large-scale or turbulent mixing. Any combination or transformation of these models can occur in a single volcanic debris avalanche, and different regimes may dominate during their transport [14]: 1) *Plug flow model*: in valley-confined settings, material can flow as a plug of coherent sliding material, with limited internal deformation, and a laminar boundary layer of highly deforming shear zones at the base and against the valley walls. Deformation happens when shear stress exceeds the yield strength of the granular mass; 2) *Translational slide model:* in unconfined or initially unconfined topography, as the avalanche initiates, listric normal faults rooted in the detaching décollement plane accommodate the initial collapse, dividing the sliding flank into the toreva domain and normal-fault-dominated upper flank, and the hummock domain and transtensional- and thrust-fault-dominated lower flank; 3) *Multiple shear zones:* pockets of shear and slip surfaces or plug zones can develop inside the debris avalanche as it moves, as a result of fragmentation of already fractured clasts, creating interclast matrix at multiple isolated locations within the moving mass. The degree of fragmentation depends on the lithology and strength of clasts [14].

Models: from initiation processes to debris avalanche distribution.

Onset of failure and geometry of debris avalanches

Scaled analogue models and numerical simulations have been used to understand how factors such as long-term fault movement, substrata, and the presence of a weak core affect the evolution and stability of volcanoes [E1, 14]. They have also been used to investigate the internal and surficial features formed after failure, during movement, and to understand the geometric, dynamic, and kinematic characteristics. In these models, scaling ensures the validity of comparisons with natural examples.

Analogue models that release sand from a trapdoor source onto a curved ramp and distinct element numerical modeling allow the observation of structures that form through brittle deformation. Normal and strike-slip faults form in areas of spreading and folds by thrust faulting are observed during deceleration. These faults converge onto a low friction sliding base [14].

Other analogue models that assume gravitational spreading at the onset of failure have two principal elements: a low viscosity basal layer, often represented by silicone, and a conical stratovolcano built of sand. At initiation, a graben perpendicular to the avalanche direction and rooted in the ductile layer forms first, and large listric normal faults converge near the base and serve as the main failure surface. The location and angle of the underlying ductile layer affect the size, depth, and steepness of the resulting failure surface and, therefore, the size of the failed mass [14]. Hummocks, which are the stretched remains of tilted and rotated blocks of the original edifice, are formed during emplacement. Their morphology depends on their original position in the initial slide and the initial structural relationships within the failed mass, and changes with spreading, breakup, or merging during emplacement. Their morphology and spatial distribution are influenced by the number of faults that form during emplacement. In model cross sections, normal faults affect the brittle upper layer, consistent with the idea that the upper brittle layer is deformed by pure shear stretching, while simple shear dominates at the base of the extending mass [14].

Dynamics and mobility of volcanic debris avalanches.

Numerical simulations offer a distinctive means to quantify the dynamics of volcanic debris avalanches and to explore the resultant tsunami generation in oceanic contexts [16]. The precise position and characteristics of the released mass, the parameters used for the numerical simulation, the rheological laws, and the approximations inherent in physically based models represent uncertainties that remain an active area of research and represent an ongoing challenge. Analogue experiments aid in constraining these uncertainties. Despite their inherent limitations, simplified depth-averaged models are frequently utilized for field-scale studies but are less accurate than full 3-D models. These simplified models rely on the thin-layer approximation for landslides and on shallow-water or long-wave approximations for tsunamis, assuming that the landslide thickness or water depth is significantly smaller than the landslide downslope extension or tsunami wavelength, respectively. Application of these models to geological cases enhances our understanding of how past flank collapses have led to their observed deposits [16]. The high fluidity of long-runout volcanic debris avalanches, characterized by runup deflection, has been simulated using depth-averaged granular flow equations and depositional features at Socompa, Chile [17]. Notably, accurately representing the effect of varying topography in simulations is crucial for obtaining deposits that are consistent with observed data. Some factors, such as event volume and the presence of an erodible substratum, significantly impact runout distance and deposit shape.
In term of hazard assessment related to seismic or volcanic activity, gravitational instabilities on steep subaerial or submarine slopes can lead to landslides, which play a significant role in the evolution of volcanoes. Numerical simulations of volcano instability and landslide-generated tsunami are thus essential as they could have a significant impact on population and infrastructure. These simulations can also help to understand the chronology and dynamics of landslides [16]. Taking into account past events and calibrating models with these parameters, or by using constraints from analogue modeling and information of the past activity, numerical simulations of debris avalanche can be used to produce maps that are useful for hazard management and planning [16] (Part 4, Chapter 3.1).

Consequences of edifice collapse

Syn-collapse eruptive scenarios: explosive activity.

Large-scale volcanic collapse abruptly removes lithostatic pressure from the magmatic and hydrothermal systems located within and beneath the edifice [2, 18]. This process may trigger syn-collapse explosive activity, the character of which depends on the interplay of two major factors. The first factor is the magnitude of the lithostatic pressure release, linked to the thickness of the failure mass removed from above the volcanic conduit. Deep-seated collapses thus induce relatively larger pressure release and may be associated with intense syn-collapse explosions or rapid accelerations in magma ascent. The second factor that determines the mechanism of the eruptive response is the internal structure of the magmatic-hydrothermal system of the collapsing edifice. Three end member responses to lateral collapse can be envisaged [18]: 1) No active hydrothermal and magmatic systems are present, and failure is thus similar to non-volcanic debris avalanches and does not trigger any syn-collapse eruptive response, (e.g., the 1800 BP collapse of Iriga volcano, Philippines); 2) There is an active hydrothermal system, but no recent magmatic activity. Collapse may induce intense phreatic explosions, as occurred in the 1888 Bandai collapse, Japan; 3) There is magma present at shallow or surficial levels, leading to syn- and post-collapse magmatic explosive eruption. The outcome of this scenario depends on the depth of the magma relative to the collapse surface (Figure 5.4.5). Laterally directed blasts can occur if the rupture surface intersects a shallow magma body (lava dome and/or cryptodome) (e.g. the 1956 Bezymianny, Kamchatka, and 1980 Mount St. Helens, USA, collapses) or vertically directed explosive eruption columns may form after collapse, where magma sits at slightly deeper levels (e.g., the 1933 Harimkotan collapse in the Kurile Islands). Laterally directed magmatic explosions (directed blasts) are the most hazardous of all syn-collapse eruptive responses because they lead to the formation of extensive devastating pyroclastic density currents (Part 3, Chapter 4.4).

Collapses may depressurize systems with more complex internal structures, triggering explosions with both phreatic and magmatic components in various proportions (e.g., the 1964 Shiveluch collapse in Kamchatka), or exposing a previously subaerial vent to seawater, resulting in sharp shifts in explosive eruption style (e.g., the Anak Krakatau, 2018, Indonesia).

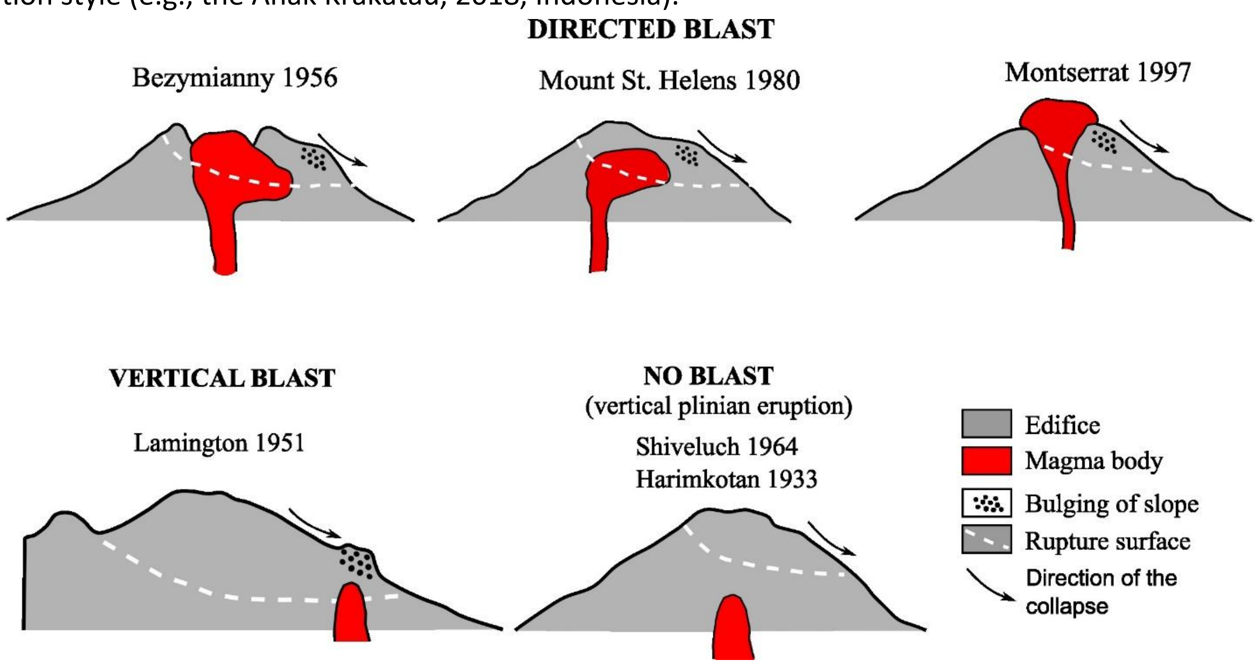

Fig. 5.4.5. Sketches illustrating the positions of magma bodies inside volcanic edifices in relation to rupture surfaces of historical gravitational collapses, and the corresponding syn-collapse explosive responses. In the case of laterally directed blasts: Bezymianny – combination of dome and cryptodome;

Mount St. Helens – cryptodome; Soufrière Hills, Montserrat – dome. At Lamington, the rupture surface intersected the uppermost part of the cryptodome (modified after [18]).

Impacts of collapse on the magmatic system.

In addition to their effects on shallowly stored magma, lateral collapses depressurize the deeper magma storage system, with a range of potential consequences [19]. These effects are dependent on the depth and geometry of stored magma and whether sufficient volumes of magma are present to be mobilised within post-collapse eruptions. Collapse does not necessarily increase the likelihood of subsequent magmatic eruptions, but there are nevertheless several examples globally where volcanic collapses have been followed by elevated eruption rates, on timescales of hundreds to thousands of years, in some cases involving distinct compositional shifts. In several cases, collapse is associated with a shift to the eruption of denser and more mafic magmas. These observations imply that lateral collapses can have long-term consequences for magma reservoirs, facilitating the ascent of magma from shallow levels and leading to replenishment from deeper levels, thus marking major eruptive cycles in the long-term (from hundreds to thousands of years) evolution of individual volcanoes. In cases where collapse induces temporarily elevated eruption rates, collapse amphitheaters can rapidly become infilled, obscuring the evidence of past lateral collapse and reestablishing a relationship between the edifice load and underlying magma system close to that which existed before collapse. Large flank collapses (> 1km^3) can lead to preferential focusing of eruptive activity within failure scars, thus forming a new cone displaced in the direction of the preceding collapse and focusing eruptive products within the collapse structure (e.g. El Reventador, Ecuador).

Post-depositional secondary processes.

Volcano lateral collapse and debris avalanche emplacement can drastically change the natural environment of the surrounding area. Lahars, triggered by water escaping from deposits (derived from groundwater or melting ice), may be initiated within hours of emplacement (e.g. Mount St. Helens), but the very large volumes of sediment introduced into the environment can result in effects that persist for years after the event, promoting sediment aggradation downstream, with a drastic consequence in distal alluvial areas. River obstructions and the formation of dams are also common effects in volcanoes flanked by deep valleys. Dam rupture can induce the formation of catastrophic lahars affecting areas hundreds of kilometers away from the original collapse source. These natural dams can last for days to years, or they can remain stable, depending on the river flow discharge or the characteristics of the obstructing material (permeability and grain size). The best examples of long-lasting (thousands of years) volcanic natural dams can be observed at Parinacota, Chile and Iriga, Philippines [20]. Some surviving lakes, such as the Coldwater and Castle Creek lakes at Mount St. Helens, are artificially controlled by a piping system to avoid water overtopping. Lacustrine sequences intercalated with volcaniclastic deposits along narrow ravines are the main evidence of the past existence of paleolakes that eventually failed, as observed for several past events at Volcán de Colima, Mexico and Chimborazo, Ecuador. A permanent river blockage can also alter the aquatic wildlife habitat. The formation of the lake can promote a stable environment for ostracod and other lacustrine species, enhance conditions for the growth of different grass species and agricultural practices that could have facilitated the settlement of ancestral populations (Part 4 Chapter 3.1).

Summary

Gravitational failures of volcanic slopes, leading to landslides and debris avalanches, are common across various volcano types and environments. These collapses can occur in both active and dormant volcanoes, influenced by factors such as the geological and tectonic settings, the internal structure of the edifice, and enhanced by volcanic or non-volcanic triggers. Volcano collapses can result in rapid, large-volume debris avalanches that cause extensive environmental damage, characterized by distinctive hummocky deposits and depicted by different lithofacies that usually reflect the internal structure of the mass prior to the collapse and the substrate. Their mobility is mainly controlled by the initial gravitational potential energy, the downslope topography, internal deformation, and basal friction during transport. Analogue and numerical models have been used to better understand factors controlling initial volcano instability and volcanic debris avalanche morphology and mobility. Such events can control the post-failure magmatic evolution of the volcano and can trigger secondary hazards such as laterally directed blasts, tsunamis, lahars, and landscape changes with significant ecological impacts. Since the timing and magnitude of such events are not always directly correlated with monitoring signals, it is crucial to deepen our understanding of volcanic debris avalanche processes, particularly in densely populated volcanic regions.

References

[1] A. Dufresne, L. Siebert, B. Bernard, Distribution and Geometric Parameters of Volcanic Debris Avalanche Deposits, in: M. Roverato, A. Dufresne, J.Procter (Eds), Volcanic Debris Avalanches. Advances in Volcanology. Springer (2021) 75-90, https://doi.org/10.1007/978-3-030-57411-6_4.
[2] L. Siebert, and M.E. Reid, Lateral edifice collapse and volcanic debris avalanches: a post-1980 Mount St. Helens perspective, *Bull. Volcanol.* **85**, 61 (2023).
[3] M. Roverato, F. Di Traglia, J. Procter, F. Paguican, A. Dufresne, Factors Contributing to Volcano Lateral Collapse, in: M. Roverato, A. Dufresne, J. Procter (Eds) Volcanic Debris Avalanches. Advances in Volcanology. Springer (2021) 91-119, https://doi.org/10.1007/978-3-030-57411-6_5.
[4] A. Belousov, M. Belousova, B. Voight, Multiple edifice failures, debris avalanches and associated eruptions in the Holocene history of Shiveluch volcano, Kamchatka, Russia. Bulletin of Volcanology 61(5) (1999) 324–342, https://doi.org/10.1007/s004450050300.
[5] van Wyk de Vries, B., Self, S., Francis, P. W., & Keszthelyi, L., A gravitational spreading origin for the Socompa debris avalanche, Journal of Volcanology and Geothermal Research 105(3) (2001) 225-247, https://doi.org/10.1016/S0377-0273(00)00252-3.

[6] T. Shea, B. van Wyk de Vries, M. Pilato, Emplacement mechanisms of contrasting debris avalanches at Volcan Mombacho (Nicaragua), provided by structural and facies analysis, Bulletin of Volcanology 70(8) (2007) 899, https://doi.org/10.1007/s00445-007-0177-7.
[7] L. Capra, J.P. Bernal, G. Carrasco-Núñez, M. Roverato, Climatic fluctuations as a significant contributing factor for volcanic collapses. Evidence from Mexico during the Late Pleistocene, Global Planet Change 100 (2013) 194–203.
[8] A. Dufresne, A. Zernack, K. Bernard, J.C. Thouret, M. Roverato, Sedimentology of Volcanic Debris Avalanche Deposits, in: M. Roverato, A. Dufresne, J. Procter (Eds), Volcanic Debris Avalanches, Advances in Volcanology, Springer (2021) 175-210, https://doi.org/10.1007/978-3-030-57411-6_8.
[9] D.R. Crandell, C.D. Miller, H.X. Glicken, R.L. Christiansen, C.G. Newhall, Catastrophic debris avalanche from ancestral Mount Shasta volcano, California, Geology 12 (1984) 143–146.
[10] H. Glicken, Sedimentary architecture of large volcanic debris avalanches, In: R.V. Fisher, G.A. Smith (Eds), Sedimentation in Volcanic Settings, SEPM special publication 45 (1991) 99–106.
[11] D.G. Masson, A.B. Watts, M.J.R. Gee, R. Urgeles, N.C. Mitchell, T.P. Le Bas, M. Canals, Slope failures on the flanks of the western Canary Islands, Earth-Sci. Rev. 57 (2002) 1–35.
[12] A. Le Friant, E. Lebas, M. Brunet, S. Lafuerza, M. Hornbach, M. Coussens et al., Submarine Landslides Around Volcanic Islands: A Review of What Can Be Learned From the Lesser Antilles Arc, in: K. Ogata, A. Festa, G.A: Pini (Eds), Submarine Landslides: Subaqueous Mass Transport Deposits from Outcrops to Seismic Profiles (2019) 277–297, doi:10.1002/9781119500513.ch17.
[13] S.F.L. Watt, P.J. Talling, J.E. Hunt, New insights into the emplacement dynamics of volcanic-island landslides, Oceanography 27 (2014) 46–57.
[14] E.M. Paguican, M. Roverato, H. Yoshida, Volcanic Debris Avalanche Transport and Emplacement Mechanisms, in: M. Roverato, A. Dufresne, J. Procter (Eds) Volcanic Debris Avalanches. Advances in Volcanology. Springer (2021) 143-173, https://doi.org/10.1007/978-3-030-57411-6_7.
[15] A. Dufresne, T.R. Davies, Longitudinal ridges in mass movement deposits, Geomorphology, 105(3-4) (2009) 171-181, https://doi.org/10.1016/j.geomorph.2008.09.009
[16] P. Poulain, A. Le Friant, A. Mangeney, S. Viroulet, E. Fernandez-Nieto, M.C. Diaz, et al., Performance and limits of a shallow-water model for landslide-generated tsunamis: from laboratory experiments to simulations of flank collapses at Montagne Pelée (Martinique), Geophysical Journal International 233(2) (2022) 796–825. https://doi.org/10.1093/gji/ggac482.
[17] K. Kelfoun, T.H. Druitt, Numerical modeling of the emplacement of Socompa rock avalanche, Chile, Journal of Geophysical Research: Solid Earth *110*(12) (2005) 1–13, https://doi.org/10.1029/2005JB003758.
[18] A. Belousov, M. Belousova, R. Hoblitt, and H. Patia, The 1951 eruption of Mount Lamington, Papua New Guinea: Devastating directed blast triggered by small-scale edifice failure, J. Volcanol. Geotherm. Res. 401, 106947 (2020).
[19] S.F.L. Watt, The evolution of volcanic systems following sector collapse, Journal of Volcanology and Geothermal Research 384 (2019) 280–303, https://doi.org/10.1016/j.jvolgeores.2019.05.012
[20] X. Fan, A. Dufresne, S.S. Subramanian, A. Strom, R. Hermanns, C.T. Stefanelli, et al., The formation and impact of landslide dams – State of the art, Earth-Science Reviews 203 (2020). 103116. https://doi.org/10.1016/j.earscirev.2020.103116.

List of References to 2015 Encyclopedia chapters

[E1] H. Sigurdsson, 2015, Chapter 38, Landslides, debris avalanches and volcanic gravitational deformations, B. van Wyk de Vries et al.

References for figures.

References fig. 5.4.1

Capra (2006) Abrupt climatic changes as triggering mechanism of massive volcanic collapses. Journal of Volcanology and Geothermal Research 155:329-333

Donnadieu F, Merle O, Besson JC (2001) Volcanic edifice stability during cryptodome intrusion. Bull. Volcanol. 63:61-72

Elseworth D, Voight B (1995) Dike intrusion as a trigger for large earthquakes and the failure of volcano flanks. J. Geo- phys. Res. 100(B4):6005-6024

McGuire WJ (1996) Volcano instability: a review of contemporary themes. Geological Society, London, Special Publications 110(1):1-23

Norini G, Agliardi F, Crosta G, Groppelli G, Zuluaga MC (2019) Structure of the Colima Volcanic Complex: Origin and Behaviour of Active Fault Systems in the Edifice, in Varley N, Connor CB, Komorowski JC (eds) Volcanic de Colima, Active Volcanoes of the World, Springer

Reid ME (2004) Massive collapse of volcano edifices triggered by hydrothermal pressurization. Geology 32(5):373-376

Roberti G, Roberts NJ, Lit C (2021) Climatic influence on volcanic landslides. In: Roverato M, Dufresne A, Procter J (eds) Volcanic dedris avalanches: from collapse to hazard. Advances in volcanology. Springer, Berlin

van Wyk de Vries B, Merle O (1996) The Effect of Volcanic Constructs on Rift Fault Patterns. Geology 24 (7): 643

Watt SF, Karstens J, Micallef A, Berndt C, Urlaub M, Ray M, Desai A, Sammartini M, Klaucke I, Böttner C, Day S, Downes H, Kühn M, Elger J (2019) From catastrophic collapse to multi-phase deposition: Flow transformation, seafloor interaction and triggered eruption following a volcanic-island landslide. Earth and Planetary Science Letters 517:135-147

Zimbelman DR, Watters RJ, Firth IR, Breit GN, Carrasco-Nuñez G (2004) Stratovolcano stability assessment methods and results from Citlaltepetl, Mexico. Bull. Volcanol. 66:66-79

References fig. 5.4.2

Bernard, B., Takarada, S., Andrade, S. D. & Dufresne, A. Terminology and strategy to describe volcanic landslides and debris avalanches. in Volcanic Debris Avalanches, From Collapse to Hazard (eds. Roverato, M., Dufresne, A. & Procter, J.) 51–73 (2021). doi:10.1007/978-3-030-57411-6_3.

Dufresne, A., & Davies, T. R. (2009). Longitudinal ridges in mass movement deposits. Geomorphology, 105(3–4), 171–181. https://doi.org/10.1016/j.geomorph.2008.09.009

Dufresne, A., Salinas, S., & Siebe, C. (2010). Substrate deformation associated with the Jocotitlán edifice collapse and debris avalanche deposit, Central México. Journal of Volcanology and Geothermal Research, 197(1–4), 133–148. https://doi.org/10.1016/j.jvolgeores.2010.02.019

Dufresne, A., Siebert, L., & Bernard, B. (2021). Distribution and Geometric Parameters of Volcanic Debris Avalanche Deposits. In M. Roveraro, A. Dufresne, & J. Procter (Eds.), Volcanic Debris Avalanches, From Collapse to Hazard, Advances in Volcanology. Springer, Cham. (pp. 75–90). https://doi.org/10.1007/978-3-030-57411-6_4

Siebe, C., Komorowski, J.-C. & Sheridan, M. F. Morphology and emplacement of an unusual debris-avalanche deposit at Jocotitlán volcano, Central Mexico. Bull. Volcanol. 54, 573–589 (1992).

References fig. 5.4.3

Caballero, L., & Capra, L. (2011). Textural analysis of particles from El Zaguán debris-avalanche deposit, Nevado de Toluca volcano, Mexico: Evidence of flow behavior during emplacement. Journal of Volcanology and Geothermal Research, 200(1–2), 75–82. https://doi.org/10.1016/j.jvolgeores.2010.12.003

Norini, G., Capra, L., Groppelli, G., & Lagmay, A. M. F. (2008). Quaternary sector collapses of Nevado de Toluca volcano (Mexico) governed by regional tectonics and volcanic evolution Quaternary sector collapses of Nevado de Toluca volcano. Geosphere, 4(5), 854–871. https://doi.org/10.1130/ges00165.1

Roverato, M., Capra, L., Sulpizio, R., & Norini, G. (2011). Stratigraphic reconstruction of two debris avalanche deposits at Colima Volcano (Mexico): Insights into pre-failure conditions and climate influence. Journal of Volcanology and Geothermal Research, 207(1–2), 33–46. https://doi.org/10.1016/j.jvolgeores.2011.07.003

References fig. 5.4.4

Brunet, M., A. Le Friant, G. Boudon, S. Lafuerza, P. Talling, M. Hornbach, O. Ishizuka, E. Lebas, H. Guyard, & IODP Expedition 340 Science Party (2016), Composition, geometry, and emplacement dynamics of a large volcanic island landslide offshore Martinique: From volcano flank- collapse to seafloor sediment failure? Geochem. Geophys. Geosyst., 17(3):699– 724, doi:10.1002/2015GC006034.

Karstens, J., Berndt, C., Urlaub, M., Watt, S.F., Micallef, A., Ray, M., Klaucke, I., Muff, S., Klaeschen, D., Kühn, M. & Roth, T. (2019). From gradual spreading to catastrophic collapse–Reconstruction of the 1888 Ritter Island volcanic sector collapse from high-resolution 3D seismic data. Earth and Planetary Science Letters, 517:1-13.

Le Friant, A., Ishizuka, O. , Boudon, G. , Palmer, M.R. , Talling, P. , Villemant, B. , Adachi, T., Aljahdali, M., Breitkreuz, C., Brunet, M., Caron, B., Coussens, M., Deplus, C., Endo, D., Feuillet, N., Fraas, A.J., Fujinawa, A., Hart, M. B., Hatfield, R.G., Hornbach, M., Jutzeler, M., Kataoka, K. S., Komorowski, J-C., Lebas, E., Lafuerza, S., Maeno, F., Manga, M., Martínez-Colón, M., McCanta, M., Morgan, S., Saito, T., Slagle, A., Sparks, S., Stinton, A., Stroncik, N., Subramanyam, K. S.V., Tamura, Y., Trofimovs, J., Voight, B., Wall-Palmer, D., Wang, F. & Watt, S.F.L. (2015). Submarine record of volcanic island construction and collapse in the Lesser Antilles arc: First scientific drilling of submarine volcanic island landslides by IODP Expedition 340. Geochem., Geophys., Geosyst, 16(2):420-442.

Lipman, P.W., Sisson, T.W., Ui, T., Naka, J. & Smith, J.R. (2002). Ancestral submarine growth of Kilauea volcano and instability of its south flank. Hawaiian volcanoes: deep underwater perspectives, 128:161-191.

Longpré, M.A., Chadwick, J.P., Wijbrans, J. & Iping, R. (2011). Age of the El Golfo debris avalanche, El Hierro (Canary Islands): New constraints from laser and furnace 40Ar/39Ar dating. Journal of Volcanology and Geothermal Research, 203(1-2):76-80.

Masson, D.G. (1996). Catastrophic collapse of the volcanic island of Hierro 15 ka ago and the history of landslides in the Canary Islands. Geology, 24(3):231-234.

Smith, J.R., Malahoff, A. and Shor, A.N., 1999. Submarine geology of the Hilina slump and morpho-structural evolution of Kilauea volcano, Hawaii. Journal of volcanology and geothermal research, 94(1-4), pp.59-88.

Ward, S.N. & Day, S. (2003). Ritter Island volcano—lateral collapse and the tsunami of 1888. Geophysical Journal International, 154(3):891-902.

Watt, S.F.L., Talling, P.J., Vardy, M.E., Masson, D.G., Henstock, T.J., Hühnerbach, V., Minshull, T.A., Urlaub, M., Lebas, E., Le Friant, A. & Berndt, C. (2012). Widespread and progressive seafloor-sediment failure following volcanic debris avalanche emplacement: Landslide dynamics and timing offshore Montserrat, Lesser Antilles. Marine Geology, 323:69-94.

Watt, S.F., Karstens, J. & Berndt, C. (2021). Volcanic-island lateral collapses and their submarine deposits. In M. Roveraro, A. Dufresne, & J. Procter (Eds.), Volcanic Debris Avalanches, From Collapse to Hazard, pp.255-279.

References fig. 5.4.5

Belousova M., Belousov A. (1995) Prehistoric and 1933 debris avalanches and associated eruptions of Harimkotan Volcano (Kurile islands). Conference: Volcanoes in Town, Rome, Periodico di Mineralogia LXIV: 99-101.

Belousov A.B. (1995). The Shiveluch volcanic eruption of 12 November 1964 - explosive eruption provoked by failure of the edifice. Journal of Volcanology and Geothermal Research, 66: 357-365

Belousov A., Belousova M. (1996) Large scale landslides on active volcanoes in XXth century - examples from Kurile-Kamchatka region (Russia). In: Landslides, Ed. Senneset K. (Balkema, Rotterdam): 953-957.

Belousov A. (1996) Pyroclastic deposits of March 30, 1956 directed blast at Bezymianny volcano. Bulletin of Volcanology, 57: 649-662.

Belousov A., Voight B., Belousova M. (2007). Directed blasts and blast-currents: a comparison of the Bezymianny 1956, Mount St Helens 1980, and Soufriere Hills, Montserrat 1997 eruptions and deposits. Bulletin of Volcanology, 69: 701-740.

Belousov A., Belousova M., Hoblitt R., Patia H. (2020). The 1951 eruption of Mount Lamington, Papua New Guinea: Devastating directed blast triggered by small-scale edifice failure. Journal of Volcanology and Geothermal Research, 401: 106947.

Voight B., Komorowski J-C., Norton G.E, Belousov A.B, Belousova M.G., Boudon G., Fransis P.W., Franz W., Heinrich P., Sparks R.S.J., Young S.R. (2002). The 26 December (Boxing Day) 1997 sector collapse and debris avalanche at Soufriere Hills Volcano, Montserrat. In Druitt, T H and Kokelaar, B P (eds), The Eruption of Soufriere Hills Volcano, Montserrat, from 1995 to 1999. Geological Society, London, Memoirs, 21: 363-407.

Further readings

Volcanic landslide: Factors contributing to volcano instability.

Andrade, S. D., & Vries, B. van W. de. (2010). Structural analysis of the early stages of catastrophic stratovolcano flank-collapse using analogue models. *Bulletin of Volcanology*, *72*(7), 771–789. https://doi.org/10.1007/s00445-010-0363-x

Andrade, S. D., Vries, B. van W. de, & Robin, C. (2019). Imbabura volcano (Ecuador): The influence of dipping-substrata on the structural development of composite volcanoes during strike-slip faulting. *Journal of Volcanology and Geothermal Research*, *385*, 68–80. https://doi.org/10.1016/j.jvolgeores.2018.11.017

Cecchi, E., Vries, B. van W. de, & Lavest, J.-M. (2004). Flank spreading and collapse of weak-cored volcanoes. *Bulletin of Volcanology*, *67*(1), 72–91. https://doi.org/10.1007/s00445-004-0369-3

Coussens, M., Wall-Palmer, D., Talling, Peter. J., Watt, Sebastian. F. L., Cassidy, M., Jutzeler, M., Clare, M. A., Hunt, James. E., Manga, M., Gernon, Thomas. M., Palmer, Martin. R., Hatter, Stuart. J., Boudon, G., Endo, D., Fujinawa, A., Hatfield, R., Hornbach, Matthew. J., Ishizuka, O., Kataoka, K., … Stinton, Adam. J. (2016). The relationship between eruptive activity, flank collapse, and sea level at volcanic islands: A long-term (>1 Ma) record offshore Montserrat, Lesser Antilles. *Geochemistry, Geophysics, Geosystems*, *17*(7), 2591–2611. https://doi.org/10.1002/2015gc006053

Delcamp, A., Vries, B. van W. de, & James, M. R. (2008). The influence of edifice slope and substrata on volcano spreading. *Journal of Volcanology and Geothermal Research*, *177*(4), 925–943. https://doi.org/10.1016/j.jvolgeores.2008.07.014

Foshag, W. P., & Gonzales, R. J. (1956). Birth and development of Paricutin volcano, Mexico. *U.S. Geological Survey Bulletin*, *965-D*, 355–487. https://pubs.usgs.gov/bul/0965d/report.pdf

Glicken, H., & Nakamura, Y. (1988). Restudy of the 1888 eruption of Bandai volcano, Japan. *Proc Kagoshima Int Conf Volcanoes, Japan*, 392–395.

Kerle, N., & Vries, B. van W. de. (2001). The 1998 debris avalanche at Casita volcano, Nicaragua — investigation of structural deformation as the cause of slope instability using remote sensing. *Journal of Volcanology and Geothermal Research*, *105*(1–2), 49–63. https://doi.org/10.1016/s0377-0273(00)00244-4

Lagmay, A. M. F., Vries, B. van W. de, Kerle, N., & Pyle, D. M. (2000). Volcano instability induced by strike-slip faulting. *Bulletin of Volcanology*, *62*(4–5), 331–346. https://doi.org/10.1007/s004450000103

Mahr, J., Harpp, K. S., Kurz, M. D., Geist, D., Bercovici, H., Pimentel, R., Cleary, Z., & Aguilar, M. D. C. (2016). Rejuvenescent Volcanism on San Cristobal Island, Galapagos: A Late ``Plumer''. *AGU Fall Meeting Abstracts*, V53C-3119. https://ui.adsabs.harvard.edu/abs/2016AGUFM.V53C3119M

McGuire, W. J. (1986). Volcano instability: a review of contemporary themes. *Geological Society, London, Special Publications*, *110*, 1–23. https://doi.org/10.1144/gsl.sp.1996.110.01.01

Norini, G., & Lagmay, A. M. F. (2005). Deformed symmetrical volcanoes. *Geology*, *33*(7), 605–608. https://doi.org/10.1130/g21565.1

Norini, G., Capra, L., Groppelli, G., Agliardi, F., Pola, A. (2010). Structural architecture of the Colima Volcanic Complex. *J. Geophys. Res.: Solid Earth,* 115, 10.1029/2010jb007649

Pioli, L., Erlund, E., Johnson, E., Cashman, K., Wallace, P., Rosi, M., & Granados, H. D. (2008). Explosive dynamics of violent Strombolian eruptions: The eruption of Parícutin Volcano 1943–1952 (Mexico). *Earth and Planetary Science Letters*, *271*(1–4), 359–368. https://doi.org/10.1016/j.epsl.2008.04.026

Roberti, G., Ward, B., Vries, B. van W. de, Friele, P., Perotti, L., Clague, J. J., & Giardino, M. (2018). Precursory slope distress prior to the 2010 Mount Meager landslide, British Columbia. *Landslides*, *15*(4), 637–647. https://doi.org/10.1007/s10346-017-0901-0

Roverato, M., Dufresne, A., & Procter, J. (2021). *Volcanic Debris Avalanches: From collapse to hazard*. Springer. https://doi.org/10.1007/978-3-030-57411-6

Siebert, L., Glicken, H., & Ui, T. (1987). Volcanic hazards from Bezymianny- and Bandai-type eruptions. *Bulletin of Volcanology*, *49*(1), 435–459. https://doi.org/10.1007/bf01046635

Stansell, N. D. (2013). Radiocarbon ages for the timing of debris avalanches at Mombacho Volcano, Nicaragua. *Bulletin of Volcanology*, *75*(1), 686. https://doi.org/10.1007/s00445-012-0686-x

Tibaldi, A., Lagmay, A. M. F. A., & Ponomareva, V. V. (2005). Effects of basement structural and stratigraphic heritages on volcano behaviour and implications for human activities (the UNESCO/IUGS/IGCP project 455). *Episodes*, *28*(3), 158–170. https://doi.org/10.18814/epiiugs/2005/v28i3/002

Tormey, D. (2010). Managing the effects of accelerated glacial melting on volcanic collapse and debris flows: Planchon–Peteroa Volcano, Southern Andes. *Global and Planetary Change*, *74*(2), 82–90. https://doi.org/10.1016/j.gloplacha.2010.08.003

Vallejo, S., Diefenbach, A. K., Gaunt, H. E., Almeida, M., Ramón, P., Naranjo, F., & Kelfoun, K. (2024). Twenty years of explosive-effusive activity at El Reventador volcano (Ecuador) recorded in its geomorphology. *Frontiers in Earth Science*, *11*, 1202285. https://doi.org/10.3389/feart.2023.1202285

Van Vries de Wyk, B., & Francis, P. W. (1997). Catastrophic collapse at stratovolcanoes induced by gradual volcano spreading. *Nature*, *387*(6631), 387–390. https://doi.org/10.1038/387387a0

Van Vries de Wyk, B., & Merle, O. (1998). Extension induced by volcanic loading in regional strike-slip zones. *Geology*, *26*(11), 983–986. https://doi.org/10.1130/0091-7613(1998)026<0983:eibvli>2.3.co;2

Van Vries de Wyk, B., Self, S., Francis, P. W., & Keszthelyi, L. (2001). A gravitational spreading origin for the Socompa debris avalanche. *Journal of Volcanology and Geothermal Research*, *105*(3), 225–247. https://doi.org/10.1016/s0377-0273(00)00252-3

Vidal, N., & Merle, O. (2000). Reactivation of basement faults beneath volcanoes: a new model of flank collapse. *Journal of Volcanology and Geothermal Research*, *99*(1–4), 9–26. https://doi.org/10.1016/s0377-0273(99)00194-8

Villeneuve, M. C., & Heap, M. J. (2021). Calculating the cohesion and internal friction angle of volcanic rocks and rock masses. *Volcanica*, *4*(2), 279–293. https://doi.org/10.30909/vol.04.02.279293

Voight, B., Glicken, H., Janda, R. J., & Douglass, M. (1981). *Catastrophic rockslide avalanche of May 18 (Mount St. Helens).* (U. S. G. S. P. Paper, Ed.; Vol. 1250).

Voight, B., Komorowski, J.-C., Norton, G. E., Belousov, A. B., Belousova, M., Boudon, G., Francis, P. W., Franz, W., Heinrich, P., Sparks, R. S. J., & Young, S. R. (2002). The 26 December (Boxing Day)

1997 sector collapse and debris avalanche at Soufrière Hills Volcano, Montserrat. *Geological Society, London, Memoirs*, *21*(1), 363–407. https://doi.org/10.1144/gsl.mem.2002.021.01.17
Wadge, G., Francis, P. W., & Ramirez, C. F. (1995). The Socompa collapse and avalanche event. *Journal of Volcanology and Geothermal Research*, *66*(1–4), 309–336. https://doi.org/10.1016/0377-0273(94)00083-s
Watt, S. F. L., Pyle, D. M., & Mather, T. A. (2013). The volcanic response to deglaciation: Evidence from glaciated arcs and a reassessment of global eruption records. *Earth-Science Reviews*, *122*, 77–102. https://doi.org/10.1016/j.earscirev.2013.03.007
White, W. M., McBirney, A. R., & Duncan, R. A. (1993). Petrology and geochemistry of the Galápagos Islands: Portrait of a pathological mantle plume. *Journal of Geophysical Research: Solid Earth*, *98*(B11), 19533–19563. https://doi.org/10.1029/93jb02018
Wooller, L., Vries, B. van W. de, Murray, J. B., Rymer, H., & Meyer, S. (2004). Volcano spreading controlled by dipping substrata. *Geology*, *32*(7), 573–576. https://doi.org/10.1130/g20472.1
Zernack, A. V. (2021). Volcanic Debris-Avalanche Deposits in the Context of Volcaniclastic Ring Plain Successions—A Case Study from Mt. Taranaki. In M. Roverato, A. Dufresne, & J. Procter (Eds.), *Volcanic Debris Avalanches, From Collapse to Hazard* (pp. 211–254). https://doi.org/10.1007/978-3-030-57411-6_9

The deposits.

Bernard, B., Takarada, S., Andrade, S. D., & Dufresne, A. (2021). Terminology and strategy to describe volcanic landslides and debris avalanches. In M. Roverato, A. Dufresne, & J. Procter (Eds.), *Volcanic Debris Avalanches, From Collapse to Hazard* (pp. 51–73). https://doi.org/10.1007/978-3-030-57411-6_3
Bernard, B., Van Vries de Wyk, B., & Leyrit, H. (2009). Distinguishing volcanic debris avalanche deposits from their reworked products: the Perrier sequence (French Massif Central). *Bulletin of Volcanology*, *71*(9), 1041. https://doi.org/10.1007/s00445-009-0285-7
Bustos, E., Norini, G., Báez, W.A., Grosse, P., Arnosio, M., Capra, L. (2024) A new remote-sensing-based volcanic debris avalanche database of Northwest Argentina (Central Andes). *Landslides* 1–20, doi:10.1007/s10346-024-02365-y.
Caballero, L., & Capra, L. (2011). Textural analysis of particles from El Zaguán debris avalanche deposit, Nevado de Toluca volcano, Mexico: Evidence of flow behavior during emplacement. *Journal of Volcanology and Geothermal Research*, *200*(1–2), 75–82. https://doi.org/10.1016/j.jvolgeores.2010.12.003
Delcamp, A., Kervyn, M., Benbakkar, M., Kwelwa, S., & Peter, D. (2017). Large volcanic landslide and debris avalanche deposit at Meru, Tanzania. *Landslides*, *14*(3), 833–847. https://doi.org/10.1007/s10346-016-0757-8
1. Dufresne, A. & Davies, T. R. (2009) Longitudinal ridges in mass movement deposits. Geomorphology 105, 171–181.
Glicken, H. (1991). Sedimentary architecture of large volcanic debris avalanches. In R. V. Fisher & G. A. Smith (Eds.), *Sedimentation in Volcanic Settings* (pp. 99–106). https://doi.org/10.2110/pec.91.45.0099
Glicken, H. (1996). *ROCKSLIDE-DEBRIS AVALANCHE OF MAY 18, 1980, MOUNT ST. HELENS VOLCANO, WASHINGTON* (U. S. D. of the I. U. S. G. Survey, Ed.). Open-file Report 96-677. chrome-

extension://efaidnbmnnnibpcajpcglclefindmkaj/https://pubs.usgs.gov/of/1996/0677/pdf/of1996-0677text.pdf
Gómez-Castillo, G., Mendoza, M. E., Macías, J. L., & Vargas-Ramírez, N. (2020). Detailed geomorphology of debris avalanches of El Estribo volcanic complex (Central Mexico). *Journal of Maps*, *16*(2), 552–564. https://doi.org/10.1080/17445647.2020.1782784
Gorshkov, G. S. (1959). Gigantic eruption of the volcano bezymianny. *Bulletin Volcanologique*, *20*(1), 77–109. https://doi.org/10.1007/bf02596572
Kerle, N., & Van Vries de Wyk, B. (2001). The 1998 debris avalanche at Casita volcano, Nicaragua — investigation of structural deformation as the cause of slope instability using remote sensing. *Journal of Volcanology and Geothermal Research*, *105*(1–2), 49–63. https://doi.org/10.1016/s0377-0273(00)00244-4
Komorowski, J.-C., Glicken, H. X., & Sheridan, M. F. (1991). Secondary electron imagery of microcracks and hackly fracture surfaces in sand-size clasts from the 1980 Mount St. Helens debris-avalanche deposit: Implications for particle-particle interactions. *Geology*, *19*(3), 261–264. https://doi.org/10.1130/0091-7613(1991)019<0261:seioma>2.3.co;2
Makris, S., Manzella, I., Cole, P., & Roverato, M. (2020). Grain size distribution and sedimentology in volcanic mass-wasting flows: implications for propagation and mobility. *International Journal of Earth Sciences*, *109*(8), 2679–2695. https://doi.org/10.1007/s00531-020-01907-8
Makris, S., Roverato, M., Dávila-Harris, P., Cole, P., & Manzella, I. (2023). Distributed stress fluidisation: Insights into the propagation mechanisms of the Abona volcanic debris avalanche (Tenerife) through a novel method for indurated deposit sedimentological analysis. *Frontiers in Earth Science*, *11*, 1177507. https://doi.org/10.3389/feart.2023.1177507
Naranjo, J. A., Romero, J., Contreras, J. P., Orihashi, Y., Scott, K., Haller, M., & Sumino, H. (2024). Rapid growth and catastrophic destruction events of Planchón Volcano, Southern Andes. Volcanica, 7(1), 21-49.
Paguican, E. M. R., Van Vries de Wyk, B., & Lagmay, A. M. F. (2014). Hummocks: how they form and how they evolve in rockslide-debris avalanches. *Landslides*, *11*(1), 67–80. https://doi.org/10.1007/s10346-012-0368-y
Reiche, P. (1937). The Toreva-Block: A Distinctive Landslide Type. *The Journal of Geology*, *45*(5), 538–548. https://doi.org/10.1086/624563
Rodríguez, I., Páez, J., Van Vries de Wyk, M.S, Van Vries de Wyk, B., & Godoy, B. (2020). Dynamics and physical parameters of the Lastarria debris avalanche, Central Andes. *Journal of Volcanology and Geothermal Research*, *402*, 106990. https://doi.org/10.1016/j.jvolgeores.2020.106990
Roverato, M., & Capra, L. (2013). Características microtexturales como indicadores del transporte y emplazamiento de dos depósitos de avalancha de escombros del Volcán de Colima (México). *Revista Mexicana de Ciencias Geologicas*, *30*(3), 512–525.
Siebert, L. (1984). Large volcanic debris avalanches: Characteristics of source areas, deposits, and associated eruptions. *Journal of Volcanology and Geothermal Research*, *22*(3–4), 163–197. https://doi.org/10.1016/0377-0273(84)90002-7
Ui, T. (1983). Volcanic dry avalanche deposits — Identification and comparison with nonvolcanic debris stream deposits. *Journal of Volcanology and Geothermal Research*, *18*(1–4), 135–150. https://doi.org/10.1016/0377-0273(83)90006-9

Voight, B., Glicken, H., Janda, R. J., & Douglass, M. (1981). *Catastrophic rockslide avalanche of May 18 (Mount St. Helens).* (U. S. G. S. P. Paper, Ed.; Vol. 1250).

Yoshida, H., Sugai, T., & Ohmori, H. (2012). Size–distance relationships for hummocks on volcanic rockslide-debris avalanche deposits in Japan. *Geomorphology*, *136*(1), 76–87. https://doi.org/10.1016/j.geomorph.2011.04.044

Instability in volcanic Island.

Belousova M., Belousov A. (1995) Prehistoric and 1933 debris avalanches and associated eruptions of Harimkotan Volcano (Kurile islands). Conference: Volcanoes in Town, Rome, Periodico di Mineralogia LXIV: 99-101.

Cassidy, M., Trofimovs, J., Watt, S. F. L., Palmer, M. R., Taylor, R. N., Gernon, T. M., Talling, P. J., & Le Friant, A. (2014). Chapter 20 Multi-stage collapse events in the South Soufrire Hills, Montserrat as recorded in marine sediment cores. *Geological Society, London, Memoirs*, *39*(1), 383–397. https://doi.org/10.1144/m39.20

Cutler, K. S., Watt, S. F. L., Cassidy, M., Madden-Nadeau, A. L., Engwell, S. L., Abdurrachman, M., Nurshal, M. E. M., Tappin, D. R., Carey, S. N., Novellino, A., Hayer, C., Hunt, J. E., Day, S. J., Grilli, S. T., Kurniawan, I. A., & Kartadinata, N. (2022). Downward-propagating eruption following vent unloading implies no direct magmatic trigger for the 2018 lateral collapse of Anak Krakatau. Earth and Planetary Science Letters, 578, 117332. https://doi.org/10.1016/j.epsl.2021.117332

Delcamp, A., Van Vries de Wyk, B., & James, M. R. (2008). The influence of edifice slope and substrata on volcano spreading. *Journal of Volcanology and Geothermal Research*, *177*(4), 925–943. https://doi.org/10.1016/j.jvolgeores.2008.07.014

Frohlich, C., Hornbach, M. J., Taylor, F. W., Shen, C.-C., Moala, 'Apai, Morton, A. E., & Kruger, J. (2009). Huge erratic boulders in Tonga deposited by a prehistoric tsunami. *Geology*, *37*(2), 131–134. https://doi.org/10.1130/g25277a.1

Garcia, M. O., Sherman, S. B., Moore, G. F., Goll, R., Popova-Goll, I., Natland, J. H., & Acton, G. (2006). Frequent landslides from Koolau Volcano: Results from ODP Hole 1223A. *Journal of Volcanology and Geothermal Research*, *151*(1–3), 251–268. https://doi.org/10.1016/j.jvolgeores.2005.07.035

Gardner, J. V. (2010). The West Mariana Ridge, western Pacific Ocean: Geomorphology and processes from new multibeam data. *GSA Bulletin*, *122*(9–10), 1378–1388. https://doi.org/10.1130/b30149.1

Hunt, J. E., Wynn, R. B., Masson, D. G., Talling, P. J., & Teagle, D. A. H. (2011). Sedimentological and geochemical evidence for multistage failure of volcanic island landslides: A case study from Icod landslide on north Tenerife, Canary Islands. *Geochemistry, Geophysics, Geosystems*, *12*(12), n/a-n/a. https://doi.org/10.1029/2011gc003740

Karstens, J., Berndt, C., Urlaub, M., Watt, S. F. L., Micallef, A., Ray, M., Klaucke, I., Muff, S., Klaeschen, D., Kühn, M., Roth, T., Böttner, C., Schramm, B., Elger, J., & Brune, S. (2019). From gradual spreading to catastrophic collapse – Reconstruction of the 1888 Ritter Island volcanic sector collapse from high-resolution 3D seismic data. *Earth and Planetary Science Letters*, *517*, 1–13. https://doi.org/10.1016/j.epsl.2019.04.009

Krastel, S., Schmincke, H., Jacobs, C. L., Rihm, R., Bas, T. P. L., & Alibés, B. (2001). Submarine landslides around the Canary Islands. *Journal of Geophysical Research: Solid Earth*, *106*(B3), 3977–3997. https://doi.org/10.1029/2000jb900413

Le Friant, A., Ishizuka, O., Boudon, G., Palmer, M. R., Talling, P. J., Villemant, B., Adachi, T., Aljahdali, M., Breitkreuz, C., Brunet, M., Caron, B., Coussens, M., Deplus, C., Endo, D., Feuillet, N., Fraas, A. J., Fujinawa, A., Hart, M. B., Hatfield, R. G., … Watt, S. F. L. (2015). Submarine record of volcanic island construction and collapse in the Lesser Antilles arc: First scientific drilling of submarine volcanic island landslides by IODP Expedition 340. *Geochemistry, Geophysics, Geosystems*, *16*(2), 420–442. https://doi.org/10.1002/2014gc005652

Le Friant, A., Lebas, E., Clément, V., Boudon, G., Deplus, C., Voogd, B. de, & Bachèlery, P. (2011). A new model for the evolution of La Réunion volcanic complex from complete marine geophysical surveys. *Geophysical Research Letters*, *38*(9). https://doi.org/10.1029/2011gl047489

Løvholt, F., Pedersen, G., & Gisler, G. (2008). Oceanic propagation of a potential tsunami from the La Palma Island. *Journal of Geophysical Research: Oceans*, *113*(C9). https://doi.org/10.1029/2007jc004603

Mitchell, N. C., Dade, W. B., & Masson, D. G. (2003). Erosion of the submarine flanks of the Canary Islands. *Journal of Geophysical Research: Earth Surface*, *108*(F1). https://doi.org/10.1029/2002jf000003

Moore, J. G., Clague, D. A., Holcomb, R. T., Lipman, P. W., Normark, W. R., & Torresan, M. E. (1989). Prodigious Submarine Landslides on the Hawaiian RIdge. *Journal of Geophysical Research*, *94*(B12), 17465–17484.

Moore, J. G., Normark, W. R., & Holcomb, R. T. (1994). Giant Hawaiian Landslides. *Annual Review of Earth and Planetary Sciences*, *22*(1), 119–144. https://doi.org/10.1146/annurev.ea.22.050194.001003

Nomanbhoy, N., & Satake, K. (1995). Generation mechanism of tsunamis from the 1883 Krakatau Eruption. *Geophysical Research Letters*, *22*(4), 509–512. https://doi.org/10.1029/94gl03219

Oehler, J.-F., Lénat, J.-F., & Labazuy, P. (2008). Growth and collapse of the Reunion Island volcanoes. *Bulletin of Volcanology*, *70*(6), 717–742. https://doi.org/10.1007/s00445-007-0163-0

Paris, R., Bravo, J. J. C., González, M. E. M., Kelfoun, K., & Nauret, F. (2017). Explosive eruption, flank collapse and megatsunami at Tenerife ca. 170 ka. *Nature Communications*, *8*(1), 15246. https://doi.org/10.1038/ncomms15246

Pinel, V., & Jaupart, C. (2000). The effect of edifice load on magma ascent beneath a volcano. *Philosophical Transactions of the Royal Society of London. Series A: Mathematical, Physical and Engineering Sciences*, *358*(1770), 1515–1532. https://doi.org/10.1098/rsta.2000.0601

Quidelleur, X., Hildenbrand, A., & Samper, A. (2008). Causal link between Quaternary paleoclimatic changes and volcanic islands evolution. *Geophysical Research Letters*, *35*(2). https://doi.org/10.1029/2007gl031849

Schneider, J.-L., Gérard, M., Schmincke, H.-U., Weaver, P. P. E., Firth, J., Baraza, J., Bristow, J. F., Brunner, C., Carey, S. N., Coakley, B., Fuller, M., Funck, T., Goldstrand, P., Herr, B., Hood, J., Howe, R., Jarvis, I., Lebreiro, S., Lindblom, S., … Wallace, P. (1997). Du volcan au sédiment: la dynamique du talus volcanoclastique sous-marin de Gran Canaria, canaries (Atlantique oriental, Leg ODP 157). *Comptes Rendus de l'Académie Des Sciences - Series IIA - Earth and Planetary Science*, *324*(11), 891–898. https://doi.org/10.1016/s1251-8050(97)82502-5

Urgeles, R., Canals, M., Baraza, J., Alonso, B., & Masson, D. (1997). The most recent megalandslides of the Canary Islands: El Golfo debris avalanche and Canary debris flow, west El Hierro Island. *Journal of Geophysical Research: Solid Earth*, *102*(B9), 20305–20323. https://doi.org/10.1029/97jb00649

Watt, S. F. L., Talling, P. J., Vardy, M. E., Heller, V., Hühnerbach, V., Urlaub, M., Sarkar, S., Masson, D. G., Henstock, T. J., Minshull, T. A., Paulatto, M., Le Friant, A., Lebas, E., Berndt, C., Crutchley, G. J., Karstens, J., Stinton, A. J., & Maeno, F. (2012). Combinations of volcanic-flank and seafloor-sediment failure offshore Montserrat, and their implications for tsunami generation. *Earth and Planetary Science Letters*, *319*, 228–240. https://doi.org/10.1016/j.epsl.2011.11.032

Watt, S. F. L., Talling, P. J., Vardy, M. E., Masson, D. G., Henstock, T. J., Hühnerbach, V., Minshull, T. A., Urlaub, M., Lebas, E., Le Friant, A., Berndt, C., Crutchley, G. J., & Karstens, J. (2012). Widespread and progressive seafloor-sediment failure following volcanic debris avalanche emplacement: Landslide dynamics and timing offshore Montserrat, Lesser Antilles. *Marine Geology*, *323*, 69–94. https://doi.org/10.1016/j.margeo.2012.08.002

Watts, A. B., & Masson, D. G. (1995). A giant landslide on the north flank of Tenerife, Canary Islands. *Journal of Geophysical Research: Solid Earth*, *100*(B12), 24487–24498. https://doi.org/10.1029/95jb02630

Debris avalanche mobility.

Andrade, S. D., & Van Vries de Wyk, B. (2010). Structural analysis of the early stages of catastrophic stratovolcano flank-collapse using analogue models. *Bulletin of Volcanology*, *72*(7), 771–789. https://doi.org/10.1007/s00445-010-0363-x

Bernard, B., Van Vries de Wyk, B., Barba, D., Leyrit, H., Robin, C., Alcaraz, S., & Samaniego, P. (2008). The Chimborazo sector collapse and debris avalanche: Deposit characteristics as evidence of emplacement mechanisms. *Journal of Volcanology and Geothermal Research*, *176*(1), 36–43. https://doi.org/10.1016/j.jvolgeores.2008.03.012

Borgia, A., & Van Vries de Wyk, B. (2003). The volcano-tectonic evolution of Concepción, Nicaragua. *Bulletin of Volcanology*, *65*(4), 248–266. https://doi.org/10.1007/s00445-002-0256-8

Cecchi, E., Van Vries de Wyk, B., & Lavest, J.-M. (2004). Flank spreading and collapse of weak-cored volcanoes. *Bulletin of Volcanology*, *67*(1), 72–91. https://doi.org/10.1007/s00445-004-0369-3

Clavero, J., Sparks, R., Huppert, H., & Dade, W. (2002). Geological constraints on the emplacement mechanism of the Parinacota debris avalanche, northern Chile. *Bulletin of Volcanology*, *64*(1), 40–54. https://doi.org/10.1007/s00445-001-0183-0

Davies, T. R., McSaveney, M. J., & Hodgson, K. A. (1999). A fragmentation-spreading model for long-runout rock avalanches. *Canadian Geotechnical Journal*, *36*(6), 1096–1110. https://doi.org/10.1139/t99-067

Glicken, H. (1996). *Rockslide-debris avalanche of may 18, 1980, Mount St. Helens volcano, Washington* (U. S. D. of the I. U. S. G. Survey, Ed.). Open-file Report 96-677. chrome-extension://efaidnbmnnnibpcajpcglclefindmkaj/https://pubs.usgs.gov/of/1996/0677/pdf/of1996-0677text.pdf

Guthrie, R. H., Friele, P., Allstadt, K., Roberts, N., Evans, S. G., Delaney, K. B., Roche, D., Clague, J. J., & Jakob, M. (2012). The 6 August 2010 Mount Meager rock slide-debris flow, Coast Mountains, British Columbia: characteristics, dynamics, and implications for hazard and risk assessment. *Natural Hazards and Earth System Sciences*, *12*(5), 1277–1294. https://doi.org/10.5194/nhess-12-1277-2012

Naranjo, J. A., & Francis, P. (1987). High velocity debris avalanche at Lastarria volcano in the north Chilean Andes. *Bulletin of Volcanology*, *49*(2), 509–514. https://doi.org/10.1007/bf01245476

Paguican, E. M. R., Van Vries de Wyk, B., & Lagmay, A. M. F. (2012). Volcano-tectonic controls and emplacement kinematics of the Iriga debris avalanches (Philippines). *Bulletin of Volcanology*, *74*(9), 2067–2081. https://doi.org/10.1007/s00445-012-0652-7

Paguican, E. M. R., Van Vries de Wyk, B., & Lagmay, A. M. F. (2014). Hummocks: how they form and how they evolve in rockslide-debris avalanches. *Landslides*, *11*(1), 67–80. https://doi.org/10.1007/s10346-012-0368-y

Palmer, B. A., & Neall, V. E. (1991). Contrasting lithofacies architecture in ring-plain deposits related to edifice construction and destruction, the Quaternary Stratford and Opunake Formations, Egmont Volcano, New Zealand. *Sedimentary Geology*, *74*(1–4), 71–88. https://doi.org/10.1016/0037-0738(91)90035-c

Roverato, M., Cronin, S., Procter, J., & Capra, L. (2015). Textural features as indicators of debris avalanche transport and emplacement, Taranaki volcano. *GSA Bulletin*, *127*(1–2), 3–18. https://doi.org/10.1130/b30946.1

Van Vries de Wyk, B., & Delcamp, A. (2015). Chapter 5. Volcanic Debris Avalanches. In T. Davies (Ed.), *Landslide Hazards, Risks and Disasters* (pp. 131–157). https://doi.org/10.1016/b978-0-12-396452-6.00005-7

Van Vries de Wyk, B., Kerle, N., & Petley, D. (2000). Sector collapse forming at Casita volcano, Nicaragua. *Geology*, *28*(2), 167–170. Van Vries de Wyk, B., Self, S., Francis, P. W., & Keszthelyi, L. (2001). A gravitational spreading origin for the Socompa debris avalanche. *Journal of Volcanology and Geothermal Research*, *105*(3), 225–247. https://doi.org/10.1016/s0377-0273(00)00252-3

Voight, B., Janda, R. J., Glicken, H., & Douglass, P. M. (2015). Discussion: Nature and mechanics of the Mount St Helens rockslide-avalanche of 18 May 1980. *Géotechnique*, *35*(3), 357–368. https://doi.org/10.1680/geot.1985.35.3.357

Voight, B., Komorowski, J.-C., Norton, G. E., Belousov, A. B., Belousova, M., Boudon, G., Francis, P. W., Franz, W., Heinrich, P., Sparks, R. S. J., & Young, S. R. (2002). The 26 December (Boxing Day) 1997 sector collapse and debris avalanche at Soufrière Hills Volcano, Montserrat. *Geological Society, London, Memoirs*, *21*(1), 363–407. https://doi.org/10.1144/gsl.mem.2002.021.01.17

Models: from initiation processes to debris avalanche distribution.

Abadie, S. M., Harris, J. C., Grilli, S. T., & Fabre, R. (2012). Numerical modeling of tsunami waves generated by the flank collapse of the Cumbre Vieja Volcano (La Palma, Canary Islands): Tsunami source and near field effects. *Journal of Geophysical Research: Oceans*, *117*(C5). https://doi.org/10.1029/2011jc007646

Acocella, V. (2005). Modes of sector collapse of volcanic cones: Insights from analogue experiments. *Journal of Geophysical Research: Solid Earth (1978–2012)*, *110*(B2). https://doi.org/10.1029/2004jb003166

Andrade, S. D., & Van Vries de Wyk, B. (2010). Structural analysis of the early stages of catastrophic stratovolcano flank-collapse using analogue models. *Bulletin of Volcanology*, *72*(7), 771–789. https://doi.org/10.1007/s00445-010-0363-x

Bouchut, F., Fernández-Nieto, E. D., Koné, E. H., Mangeney, A., & Narbona-Reina, G. (2021). Dilatancy in dry granular flows with a compressible μ(I) rheology. *Journal of Computational Physics*, *429*, 110013. https://doi.org/10.1016/j.jcp.2020.110013

Bougouin, A., Paris, R., & Roche, O. (2020). Impact of Fluidized Granular Flows into Water: Implications for Tsunamis Generated by Pyroclastic Flows. *Journal of Geophysical Research: Solid Earth*, *125*(5). https://doi.org/10.1029/2019jb018954
Bougouin, A., Roche, O., Paris, R., & Huppert, H. E. (2021). Experimental Insights on the Propagation of Fine-Grained Geophysical Flows Entering Water. *Journal of Geophysical Research: Oceans*, *126*(4). https://doi.org/10.1029/2020jc016838
Branquet, Y., & Van Vries de Wyk, B. (2001). Effets de la charge des édifices volcaniques sur la propagation de structures régionales compressives : exemples naturels et modèles expérimentaux. *Comptes Rendus de l'Académie Des Sciences - Series IIA - Earth and Planetary Science*, *333*(8), 455–461. https://doi.org/10.1016/s1251-8050(01)01660-3
Brunet, M., Moretti, L., Le Friant, A., Mangeney, A., Nieto, E. D. F., & Bouchut, F. (2017). Numerical simulation of the 30–45 ka debris avalanche flow of Montagne Pelée volcano, Martinique: from volcano flank collapse to submarine emplacement. *Natural Hazards*, *87*(2), 1189–1222. https://doi.org/10.1007/s11069-017-2815-5
Byrne, P. K., Holohan, E. P., Kervyn, M., Vries, B. van W. de, Troll, V. R., & Murray, J. B. (2013). A sagging-spreading continuum of large volcano structure. *Geology*, *41*(3), 339–342. https://doi.org/10.1130/g33990.1
Cecchi, E., Vries, B. van W. de, & Lavest, J.-M. (2004). Flank spreading and collapse of weak-cored volcanoes. *Bulletin of Volcanology*, *67*(1), 72–91. https://doi.org/10.1007/s00445-004-0369-3
Clavero, J., Sparks, R., Huppert, H., & Dade, W. (2002). Geological constraints on the emplacement mechanism of the Parinacota debris avalanche, northern Chile. *Bulletin of Volcanology*, *64*(1), 40–54. https://doi.org/10.1007/s00445-001-0183-0
Dartevelle, S., Rose, W. I., Stix, J., Kelfoun, K., & Vallance, J. W. (2004). Numerical modeling of geophysical granular flows: 2. Computer simulations of plinian clouds and pyroclastic flows and surges. *Geochemistry, Geophysics, Geosystems*, *5*(8). https://doi.org/10.1029/2003gc000637
Delannay, R., Valance, A., Mangeney, A., Roche, O., & Richard, P. (2017). Granular and particle-laden flows: from laboratory experiments to field observations. *Journal of Physics D: Applied Physics*, *50*(5), 053001. https://doi.org/10.1088/1361-6463/50/5/053001
Delcamp, A., Van Vries de Wyk, B., James, M. R., Gailler, L. S., & Lebas, E. (2012). Relationships between volcano gravitational spreading and magma intrusion. *Bulletin of Volcanology*, *74*(3), 743–765. https://doi.org/10.1007/s00445-011-0558-9
Delgado-Sánchez, J. M., Bouchut, F., Fernández-Nieto, E. D., Mangeney, A., & Narbona-Reina, G. (2020). A two-layer shallow flow model with two axes of integration, well-balanced discretization and application to submarine avalanches. *Journal of Computational Physics*, *406*, 109186. https://doi.org/10.1016/j.jcp.2019.109186
Edwards, A. N., Viroulet, S., Kokelaar, B. P., & Gray, J. M. N. T. (2017). Formation of levees, troughs and elevated channels by avalanches on erodible slopes. *Journal of Fluid Mechanics*, *823*, 278–315. https://doi.org/10.1017/jfm.2017.309
Fernández-Nieto, E. D., Garres-Díaz, J., Mangeney, A., & Narbona-Reina, G. (2016). A multilayer shallow model for dry granular flows with the -rheology: application to granular collapse on erodible beds. *Journal of Fluid Mechanics*, *798*, 643–681. https://doi.org/10.1017/jfm.2016.333
Fernández-Nieto, E. D., Garres-Díaz, J., Mangeney, A., & Narbona-Reina, G. (2018). 2D granular flows with the μ(I) rheology and side walls friction: A well-balanced multilayer discretization. *Journal of Computational Physics*, *356*, 192–219. https://doi.org/10.1016/j.jcp.2017.11.038

Fine, I. V., Rabinovich, A. B., Bornhold, B. D., Thomson, R. E., & Kulikov, E. A. (2005). The Grand Banks landslide-generated tsunami of November 18, 1929: preliminary analysis and numerical modeling. *Marine Geology*, *215*(1–2), 45–57. https://doi.org/10.1016/j.margeo.2004.11.007

Haas, T. de, Braat, L., Leuven, J. R. F. W., Lokhorst, I. R., & Kleinhans, M. G. (2015). Effects of debris flow composition on runout, depositional mechanisms, and deposit morphology in laboratory experiments. *Journal of Geophysical Research: Earth Surface*, *120*(9), 1949–1972. https://doi.org/10.1002/2015jf003525

Iverson, R. M., & George, D. L. (2014). A depth-averaged debris-flow model that includes the effects of evolving dilatancy. I. Physical basis. *Proceedings of the Royal Society A: Mathematical, Physical and Engineering Sciences*, *470*(2170), 20130819. https://doi.org/10.1098/rspa.2013.0819

Kelfoun, K., & Druitt, T. H. (2005). Numerical modeling of the emplacement of Socompa rock avalanche, Chile. *Journal of Geophysical Research: Solid Earth*, *110*(B12). https://doi.org/10.1029/2005jb003758

Kelfoun, K., Giachetti, T., & Labazuy, P. (2010). Landslide-generated tsunamis at Réunion Island. *Journal of Geophysical Research: Earth Surface*, *115*(F4). https://doi.org/10.1029/2009jf001381

Lagmay, A. M. F., Van Vries de Wyk, B., Kerle, N., & Pyle, D. M. (2000). Volcano instability induced by strike-slip faulting. *Bulletin of Volcanology*, *62*(4–5), 331–346. https://doi.org/10.1007/s004450000103

Lucas, A., Mangeney, A., Mège, D., & Bouchut, F. (2011). Influence of the scar geometry on landslide dynamics and deposits: Application to Martian landslides. *Journal of Geophysical Research: Planets*, *116*(E10). https://doi.org/10.1029/2011je003803

Ma, G., Kirby, J. T., Hsu, T.-J., & Shi, F. (2015). A two-layer granular landslide model for tsunami wave generation: Theory and computation. *Ocean Modelling*, *93*, 40–55. https://doi.org/10.1016/j.ocemod.2015.07.012

Mangeney, A., Bouchut, F., Thomas, N., Vilotte, J. P., & Bristeau, M. O. (2007). Numerical modeling of self-channeling granular flows and of their levee-channel deposits. *Journal of Geophysical Research: Earth Surface (2003–2012)*, *112*(F2). https://doi.org/10.1029/2006jf000469

Mangeney, A., Tsimring, L. S., Volfson, D., Aranson, I. S., & Bouchut, F. (2007). Avalanche mobility induced by the presence of an erodible bed and associated entrainment. *Geophysical Research Letters*, *34*(22). https://doi.org/10.1029/2007gl031348

Merle, O., Vidal, N., & Van Vries de Wyk, B. (2001). Experiments on vertical basement fault reactivation below volcanoes. *Journal of Geophysical Research: Solid Earth*, *106*(B2), 2153–2162. https://doi.org/10.1029/2000jb900352

Paguican, E. M. R., Van Vries de Wyk, B., & Lagmay, A. M. F. (2014). Hummocks: how they form and how they evolve in rockslide-debris avalanches. *Landslides*, *11*(1), 67–80. https://doi.org/10.1007/s10346-012-0368-y

Paris, A., Heinrich, P., Paris, R., & Abadie, S. (2020). The December 22, 2018 Anak Krakatau, Indonesia, Landslide and Tsunami: Preliminary Modeling Results. *Pure and Applied Geophysics*, *177*(2), 571–590. https://doi.org/10.1007/s00024-019-02394-y

Perttu, A., Caudron, C., Assink, J. D., Metz, D., Tailpied, D., Perttu, B., Hibert, C., Nurfiani, D., Pilger, C., Muzli, M., Fee, D., Andersen, O. L., & Taisne, B. (2020). Reconstruction of the 2018 tsunamigenic flank collapse and eruptive activity at Anak Krakatau based on eyewitness reports,

seismo-acoustic and satellite observations. *Earth and Planetary Science Letters*, *541*, 116268. https://doi.org/10.1016/j.epsl.2020.116268
Peruzzetto, M., Komorowski, J.-C., Le Friant, A., Rosas-Carbajal, M., Mangeney, A., & Legendre, Y. (2019). Modeling of partial dome collapse of La Soufrière of Guadeloupe volcano: implications for hazard assessment and monitoring. *Scientific Reports*, *9*(1), 13105. https://doi.org/10.1038/s41598-019-49507-0
Peruzzetto, M., Mangeney, A., Bouchut, F., Grandjean, G., Levy, C., Thiery, Y., & Lucas, A. (2021). Topography Curvature Effects in Thin-Layer Models for Gravity-Driven Flows Without Bed Erosion. *Journal of Geophysical Research: Earth Surface*, *126*(4). https://doi.org/10.1029/2020jf005657
Peruzzetto, M., Mangeney, A., Grandjean, G., Levy, C., Thiery, Y., Rohmer, J., & Lucas, A. (2020). Operational Estimation of Landslide Runout: Comparison of Empirical and Numerical Methods. *Geosciences*, *10*(11), 424. https://doi.org/10.3390/geosciences10110424
Pitman, E. B., & Le, L. (2005). A two-fluid model for avalanche and debris flows. *Philosophical Transactions of the Royal Society A: Mathematical, Physical and Engineering Sciences*, *363*(1832), 1573–1601. https://doi.org/10.1098/rsta.2005.1596
Poulain, P., Le Friant, A., Mangeney, A., Viroulet, S., Fernandez-Nieto, E., Diaz, M. C., Peruzzetto, M., Grandjean, G., Bouchut, F., Pedreros, R., & Komorowski, J.-C. (2022). Performance and limits of a shallow-water model for landslide-generated tsunamis: from laboratory experiments to simulations of flank collapses at Montagne Pelée (Martinique). *Geophysical Journal International*, *233*(2), 796–825. https://doi.org/10.1093/gji/ggac482
Poulain, P., Le Friant, A., Pedreros, R., Mangeney, A., Filippini, A. G., Grandjean, G., Lemoine, A., Fernández-Nieto, E. D., Díaz, M. J. C., & Peruzzetto, M. (2022). Numerical simulation of submarine landslides and generated tsunamis: application to the on-going Mayotte seismo-volcanic crisis. *Comptes Rendus. Géoscience*, *354*(S2), 1–30. https://doi.org/10.5802/crgeos.138
Pouliquen, O., & Forterre, Y. (2002). Friction law for dense granular flows: application to the motion of a mass down a rough inclined plane. *Journal of Fluid Mechanics*, *453*, 133–151. https://doi.org/10.1017/s0022112001006796
Rauter, M., Viroulet, S., Gylfadóttir, S. S., Fellin, W., & Løvholt, F. (2022). Granular porous landslide tsunami modelling – the 2014 Lake Askja flank collapse. *Nature Communications*, *13*(1), 678. https://doi.org/10.1038/s41467-022-28296-7
Robbe-Saule, M., Morize, C., Henaff, R., Bertho, Y., Sauret, A., & Gondret, P. (2020). Experimental investigation of tsunami waves generated by granular collapse into water. *Journal of Fluid Mechanics*, *907*, A11. https://doi.org/10.1017/jfm.2020.807
Savage, S. B., & Hutter, K. (1989). The motion of a finite mass of granular material down a rough incline. *Journal of Fluid Mechanics*, *199*, 177–215. https://doi.org/10.1017/s0022112089000340
Shea, T., & Van Vries de Wyk, B. (2008). Structural analysis and analogue modeling of the kinematics and dynamics of rockslide avalanchesShea and van Wyk de Vries. *Geosphere*, *4*(4), 657–686. https://doi.org/10.1130/ges00131.1
Shea, T., Van Vries de Wyk, B., & Pilato, M. (2007). Emplacement mechanisms of contrasting debris avalanches at Volcán Mombacho (Nicaragua), provided by structural and facies analysis. *Bulletin of Volcanology*, *70*(8), 899. https://doi.org/10.1007/s00445-007-0177-7
Thompson, N., Bennett, M. R., & Petford, N. (2010). Development of characteristic volcanic debris avalanche deposit structures: New insight from distinct element simulations. *Journal of*

Volcanology and Geothermal Research, *192*(3–4), 191–200. https://doi.org/10.1016/j.jvolgeores.2010.02.021
Tibaldi, A., Corazzato, C., Kozhurin, A., Lagmay, A. F. M., Pasquarè, F. A., Ponomareva, V. V., Rust, D., Tormey, D., & Vezzoli, L. (2008). Influence of substrate tectonic heritage on the evolution of composite volcanoes: Predicting sites of flank eruption, lateral collapse, and erosion. *Global and Planetary Change*, *61*(3–4), 151–174. https://doi.org/10.1016/j.gloplacha.2007.08.014
Tibaldi, A., & Lagmay, A. M. F. (2006). Interaction between volcanoes and their basement. *Journal of Volcanology and Geothermal Research*, *158*(1–2), 1–5. https://doi.org/10.1016/j.jvolgeores.2006.04.011
Van Vries de Wyk, B., & Francis, P. W. (1997). Catastrophic collapse at stratovolcanoes induced by gradual volcano spreading. *Nature*, *387*(6631), 387–390. https://doi.org/10.1038/387387a0
S. Yavari-Ramshe, B. Ataie-Ashtiani, Numerical modeling of subaerial and submarine landslide-generated tsunami waves—recent advances and future challenges, Landslides, 13 (2016) 1325–1368.
Wooller, L., Vries, B. van W. de, Cecchi, E., & Rymer, H. (2009). Analogue models of the effect of long-term basement fault movement on volcanic edifices. *Bulletin of Volcanology*, *71*(10), 1111–1131. https://doi.org/10.1007/s00445-009-0289-3

Consequences of edifice collapse.

Belousov, A. B. (1995). The Shiveluch volcanic eruption of 12 November 1964—explosive eruption provoked by failure of the edifice. *Journal of Volcanology and Geothermal Research*, *66*(1–4), 357–365. https://doi.org/10.1016/0377-0273(94)00072-o
Belousov, A., Belousova, M., & Listanco, E. (2023). Late Holocene edifice collapse and eruptions of Iriga volcano, Philippines: integrated data from subaerial and lacustrine deposits. *Bulletin of Volcanology*, *85*(7), 40. https://doi.org/10.1007/s00445-023-01653-0
Belousov, A., Voight, B., & Belousova, M. (2007). Directed blasts and blast-generated pyroclastic density currents: a comparison of the Bezymianny 1956, Mount St Helens 1980, and Soufrière Hills, Montserrat 1997 eruptions and deposits. *Bulletin of Volcanology*, *69*(7), 701. https://doi.org/10.1007/s00445-006-0109-Y
Belousov A., Belousova M., Hoblitt R., Patia H. (2020). The 1951 eruption of Mount Lamington, Papua New Guinea: Devastating directed blast triggered by small-scale edifice failure. Journal of Volcanology and Geothermal Research, 401: 106947 https://doi.org/10.1016/j.jvolgeores.2020.106947
Capra, L. (2007). Volcanic natural dams: identification, stability, and secondary effects. *Natural Hazards*, *43*(1), 45–61. https://doi.org/10.1007/s11069-006-9101-2
Capra, L., & Macías, J. L. (2002). The cohesive Naranjo debris-flow deposit (10 km3): A dam breakout flow derived from the Pleistocene debris-avalanche deposit of Nevado de Colima Volcano (México). *Journal of Volcanology and Geothermal Research*, *117*(1–2), 213–235. https://doi.org/10.1016/s0377-0273(02)00245-7
Capra, L., Roverato, M., Bernal, J. P., & Cortés, A. (2021). Evidence of the Early Holocene eruptive activity of Volcán de Colima and the 8.2 kyr global climatic event in lacustrine sediments from a debris avalanche-dammed lake. *Geological Society, London, Special Publications*, *520*(1), 477–490. https://doi.org/10.1144/sp520-2021-63

Cutler, K. S., Watt, S. F. L., Cassidy, M., Madden-Nadeau, A. L., Engwell, S. L., Abdurrachman, M., Nurshal, M. E. M., Tappin, D. R., Carey, S. N., Novellino, A., Hayer, C., Hunt, J. E., Day, S. J., Grilli, S. T., Kurniawan, I. A., & Kartadinata, N. (2022). Downward-propagating eruption following vent unloading implies no direct magmatic trigger for the 2018 lateral collapse of Anak Krakatau. *Earth and Planetary Science Letters*, *578*, 117332. https://doi.org/10.1016/j.epsl.2021.117332

Dale, V. H., & Denton, E. M. (2018). *Ecological Responses at Mount St. Helens: Revisited 35 years after the 1980 Eruption*. 149–164. https://doi.org/10.1007/978-1-4939-7451-1_8

Dale, V. H., Swanson, F. J., & Crisafulli, C. M. (2005). *Ecological Responses to the 1980 Eruption of Mount St. Helens*. 277–286. https://doi.org/10.1007/0-387-28150-9_19

Dávila-Harris, P., Branney, M. J., & Storey, M. (2011). Large eruption-triggered ocean-island landslide at Tenerife: Onshore record and long-term effects on hazardous pyroclastic dispersal. Geology, 39(10), 951-954. https://doi.org/10.1130/G31994.1

Michel, A. P., Rull, J., Aluja, M., & Feder, J. L. (2007). The genetic structure of hawthorn-infesting Rhagoletis pomonella populations in Mexico: implications for sympatric host race formation. *Molecular Ecology*, *16*(14), 2867–2878. https://doi.org/10.1111/j.1365-294x.2007.03263.x

Pinel, V., & Albino, F. (2013). Consequences of volcano sector collapse on magmatic storage zones: Insights from numerical modeling. *Journal of Volcanology and Geothermal Research*, *252*, 29–37. https://doi.org/10.1016/j.jvolgeores.2012.11.009

Romero, J. E., Moreno, H., Polacci, M., Burton, M., & Guzmán, D. (2022). Mid-Holocene lateral collapse of Antuco volcano (Chile): debris avalanche deposit features, emplacement dynamics, and impacts. Landslides, 19(6), 1321–1338. https://doi.org/10.1007/s10346-022-01865-z

Romero, J. E., Polacci, M., Arzilli, F., Schipper, C. I., Spina, G. L., Burton, M., Parada, M. A., Norambuena, J., Guevara, A., Watt, S., Moreno, H., Franco, L., & Fellowes, J. (2023). Long-term volcano evolution controlled by lateral collapse at Antuco volcano, southern Andes, Chile. Communications Earth & Environment, 4(1), 292. https://doi.org/10.1038/s43247-023-00931-1

Romero, J. E., Polacci, M., Watt, S., Kitamura, S., Tormey, D., Sielfeld, G., Arzilli, F., Spina, G. L., Franco, L., Burton, M., & Polanco, E. (2021). Volcanic Lateral Collapse Processes in Mafic Arc Edifices: A Review of Their Driving Processes, Types and Consequences. Frontiers in Earth Science, 9, 639825. https://doi.org/10.3389/feart.2021.639825

Watt, S. F. L. (2019). The evolution of volcanic systems following sector collapse. *Journal of Volcanology and Geothermal Research*, *384*, 280–303. https://doi.org/10.1016/j.jvolgeores.2019.05.012

Zizumbo-Villarreal, D., & Colunga-GarcíaMarín, P. (2010). Origin of agriculture and plant domestication in West Mesoamerica. *Genetic Resources and Crop Evolution*, *57*(6), 813–825. https://doi.org/10.1007/s10722-009-9521-4

Zizumbo-Villarreal, D., González-Zozaya, F., Olay-Barrientos, A., Platas-Rui, R., Cuevas-Sagardí, M., Almendros-López, L., & García-Marín, P. C. (2010). Importancia cultural precolombina del Agave spp. en el valle de Colima. *Arqueologia*, *40*, 179–195. https://revistas.inah.gob.mx/index.php/arqueologia/article/view/3477/3361

Zizumbo-Villarreal, D., González-Zozaya, F., Olay-Barrientos, A., Platas-Ruíz, R., Cuevas-Sagardí, M., Almendros-López, L., & Colunga-GarcíaMarín, P. (2009). Archaeological Evidence of the Cultural Importance of Agave spp. in Pre-Hispanic Colima, Mexico. *Economic Botany*, *63*(3), 288–302. https://doi.org/10.1007/s12231-009-9092-5